TK, 1N/91

Iogenic Plasma and its Rotation-Driven Transport in Jupiter's Magnetosphere

William H. Smyth

Atmospheric and Environmental Research, Inc.
131 Hartwell Avenue
Lexington, MA 02421-3126

Final Report for the Period of
September 25, 1997 to September 24, 2001

I. Introduction

In this project, research has focused upon studies for the heavy-ion-dominated plasma torus (O^+, O^{++}, S^+, S^{++}, S^{+++}, S^{++++}) and its near plasma sheet extension produced by the ionization of neutral gases from Io. Specifically, we have undertaken explicit studies and calculations to describe the spatial nature of the Iogenic plasma source and have begun to study its outward rotation-driven transport pattern in Jupiter's magnetosphere in order to identify and understand the space plasma phenomena that shape it into the Io plasma torus. The approach has been to combine state-of-the-art calculations at AER for the Iogenic plasma source and numerical solutions of the nonlinear transport equations in a collaborative effort with Drs. T. W. Hill, R. A. Wolf and colleagues at Rice University using the Rice Convection Model for Jupiter (RCM-J). In this way, we have begun to address the complex plasma torus structures that emerge from the source and transport processes.

The RCM-J's use of a fine two-dimensional grid and its many-fluid representations of the plasma make it capable of representing this complex region. The calculation of a continuous/spacetime-dependent Iogenic plasma source in three-dimensions and its proper interface with the RCM-J provide a critical and, up to now, missing element for this convection model. The Iogenic plasma source model is quite sophisticated and contains, for example, east-west and System III longitudinal asymmetries in the spacetime description of the plasma torus. The many different observational data that are carefully crafted together in determining the nature of the Iogenic plasma source have brought a required reality to this convection model that is necessary to unravel the structure and transport physics of the plasma torus. These numerical simulations are ultimately intended both to clarify the conditions for validity of various theoretical scenarios and to provide a useful tool for interpretation of plasma torus structures and *in situ* and remote data acquired by Galileo.

II. Overview of Work Performed in the Project

2.1 Iogenic Plasma Source

The Iogenic plasma source can be divided into two regions. First, there is a very spatially confined and denser "Inner Region" below Io's exobase where pickup (i.e., both electron impact ionization and charge exchange) ions are created in the local atmosphere and also where Pedersen and Hall conductivities become important in the collisionally bound ionosphere. Second there is a spatially extended but less dense "Outer Region" above the exobase created by

neutral gases from Io in the bound corona and in the more distant escaping neutral clouds where pickup ions are also created. The solution of the Iogenic plasma source for the small "Inner Region" is very complex and involves the coupling of the atmospheric structure to the electrodynamic interaction problem. The recent modeling of Saur et al. (1999) explicitly concentrated on this Inner Region with the primary purpose of solving the electrodynamic problem but with a fixed spherically symmetric atmosphere. The strength of the Iogenic plasma source for the Inner Region (effectively a point source on the broader circumplanetary scale) is thought to be comparable to and even likely larger than the Iogenic plasma source for the Outer Region. It is the volumetrically-concentrated Iogenic plasma source for the Inner Region that is now recognized (Smyth and Marconi 1998; Hill and Pontius 1998; Delamere et al. 2001) to be the dominant plasma source for creating the main density peak in the plasma torus, the so-called plasma ribbon, that is located at western elongation at ~5.7 Jupiter radius.

The primary research undertaken in this project has been to investigate the circumplanetary nature and the near-Io nature of the Iogenic plasma source for the Outer Region. The general nature of the Iogenic plasma source for the Outer Region was deduced earlier by Marconi and Smyth (1996). They noted that the nominal lifetimes (~1 to 20 hrs) for neutrals (H, O, S, SO, SO_2) in the plasma torus [due to electron impact ionization (or dissociation) and/or charge exchange reactions] are short compared to the characteristic time of ~200 hrs for neutrals to form a complete 360° toroidal cloud about Jupiter at Io's orbit. This rapid destruction of the neutral clouds in the torus hence produces a spatially extended but rather circumplanetary asymmetrically Iogenic plasma source both upstream and downstream of Io that has a large peak at the satellite's location. In this project, the Iogenic plasma source for the Outer Region has been calculated using the AER Neutral Cloud Model. The spatial nature of the Iogenic plasma source created by atomic oxygen and atomic sulfur species in the Outer Region has been calculated in three dimensions and investigated in detail both on a circumplanetary scale and on a near-Io scale for one location of Io in local time. These calculations are discussed in Section III and are presented in two companion papers: "Nature of the Iogenic Plasma Source in Jupiter's Magnetosphere I. Circumplanetary Distribution" (in appendix; Smyth and Marconi 2001a) and "Nature of the Iogenic Plasma Source in Jupiter's Magnetosphere II. Near Io Distribution" (in preparation, Smyth and Marconi 2001b).

2.2 RCM-J Transport Calculations

The original RCM-J model (Yang 1992; Yang et al. 1992, 1994; Pontius et al. 1998) has been improved during this project with the collaborative project at Rice University so as to include a space-time dependent Iogenic plasma source. This inclusion of the Iogenic plasma source has required a major revision and testing at Rice University of the earlier model code. In the improvement of this model, many unforeseen difficulties have been encountered. Although significant progress has been made, the advancement has been much more difficult and slower than initially expected.

The spatial nature of the Iogenic plasma source developed in this project has been made available to Rice University for the purpose of being incorporated into the RCM-J transport calculations. For the stage of development that the RCM-J has achieved during this project, however, the three-dimensional circumplanetary and near-Io distributions developed at AER contain too much spatial realism for the present state of the model to incorporate, although progress in the past year has been moving forward at a faster pace. A summary of the new calculations incorporating various physical elements of the Iogenic plasma source is presented in Section IV.

III. Model Calculations for the Iogenic Plasma Source in the Outer Region

3.1 Introduction

Efforts have been focused upon the investigation of the nature of the Iogenic plasma source for the Outer Source on two different spatial scales: (1) on a circumplanetary Jovicentric scale including all of Io's circular orbit (radius of ~5.9 R_J) around Jupiter and covering the radial interval from 4 to 10 R_J, and (2) on a near-Io scale for distances from the nominal exobase of 1.4 Io radii (R_{Io}) radially outward including the Lagrange sphere (radius ~5.85 R_{Io}) to a distance of ~±20 R_{Io} [i.e., ~±0.5 Jupiter radii (R_J)] from Io. These calculations have been undertaken using the *AER Neutral Cloud Model*. Efforts have been focused upon the Iogenic plasma source that are created only in the Outer Region by O and S atoms ejected from Io's exobase. The calculations are restricted to O and S since they are known to exist and have exobase source

estimates that are more certain. In these calculations, the incomplete collisional cascade source velocity distribution that was deduced for Na at Io's exobase by Smyth and Combi (1997) has been adopted for the shape of the O and S source velocity distributions at Io's exobase. An isotropic source rate at Io's exobase of 3.2 x 10^{27} atoms s^{-1} was initially adopted for O at an assumed exobase radius of 2600 km and was determined from energetic monoenergetic modeling efforts of Smyth (1992). The S source rate was initially assumed to be 1.6 x 10^{27} atoms s^{-1}, half of the O source rate, as would be consistent for a parent molecule SO_2. Later in the project, however, more realistic O and S source rates of 1.38 x 10^{28} s^{-1} and 0.69 x 10^{28} s^{-1}, about ~4 times larger than the earlier rates, were adopted. These new rates were based upon the more recent modeling of O neutral clouds by Smyth and Marconi (2000) that adopted for O the incomplete collisional cascade source velocity distributions deduced for Na at Io's exobase by Smyth and Combi (1997). All calculations discussed below were undertaken for Io located at western elongation (i.e., a geocentric phase angle of 270°, which is assumed to be at the local time of the dusk ansa) and at an Io System III longitude of 230°, so that it is well north of the centrifugal equator symmetry plane of the plasma torus and has a magnetic off-set tilted dipole L value of 5.88.

3.2 Summary of the Spatial Nature of the Iogenic Plasma Source: Circumplanetary Scale

Calculations have been performed on a circumplanetary scale about Jupiter to study the asymmetric spatial longitudinal and radial asymmetric nature of the O and S neutral densities and the ion pickup rates that they create in the proximity of Io's orbit. For this large spatial scale, the O and S neutral densities have been integrated perpendicular to Io's orbit plane to produce a two-dimensional distribution with a spatial resolution box size of (2 x 10^4) x (2 x 10^4) km. The instantaneous ion pickup rates have been integrated along the magnetic field lines to produce a two-dimensional distribution in the plasma torus centrifugal plane with an angular longitudinal resolution of 5° and a radial resolution of 0.1 R_J in the radial interval from 4 to 10 R_J.

Only a brief summary of the paper "Nature of the Iogenic Plasma Source in Jupiter's Magnetosphere I. Circumplanetary Distribution" is given here, since the paper is included in the appendix. Two-dimensional distributions produced by integrating the three-dimensional

information along the magnetic field lines are presented for the pickup ion rates, the net-mass and total-mass loading rates, the mass per unit magnetic flux rate, the pickup conductivity, the radial pickup current, and the net-energy loading rate for the plasma torus. All of the two-distributions are highly peaked at Io's location and hence highly asymmetric about Jupiter. The physical origin and the amount of asymmetry for these volumetric quantities are discussed. The spatially integrated rates for the net-mass and total-mass loading rates are 154 kg s^{-1} and 277 kg s^{-1}, respectively, with 71% of the rate confined to a very large peak located within ±20° longitude of Io's orbital location. The spatially integrated rate for the mass per unit magnetic flux is 1.1 x 10^8 kg s^{-1} T^{-1}. Maximum values for the pickup conductivity and the radial pickup current at Io's location are 2.5 x 10^{-3} mho and 4 x 10^4 amps. The spatially integrated net-energy loading rate is 1.03 x 10^{12} watts and is dominated by the contributions from the peak centered on Io.

The space-time variability of the Iogenic plasma source is discussed and is shown to depend upon the complete time history of the neutral clouds from which they are created. The Iogenic plasma source calculated here for the Outer Region is compared to various estimates for the Iogenic plasma source created in the combined Inner and Outer Regions. The mass source rate for the Inner Region is estimated to be ~300-700 kg s^{-1}, about 1 to 2.5 times larger than that calculated for the Outer Region (277 kg s^{-1}). Other possible sources of pickup ions for the Outer Region are also discussed. The Inner Region is therefore expected to be the dominant contributor of ions to the formation of the plasma torus ribbon, the maximum density peak in the radial structure of the plasma torus, and to be a comparable if not larger contributor to the energy budget of the plasma torus. Future improvements in calculating the Iogenic plasma source include the addition of near-Io plasma effects in the satellite flank and plasma wake and the more complete specification of source rates for neutrals at Io's exobase.

3.3 Spatial Nature of the Iogenic Plasma Source: Near-Io Scale

Since the Iogenic plasma source is shown in Section 3.2 to be very highly peaked at Io's instantaneous position, we have undertaken near-Io scale calculations of much higher spatial resolution to investigate the behavior of the large spatial gradients near the satellite. Calculations presented below are for the initial neutral source rates noted in Section 3.1. Calculations in the

paper "Nature of the Iogenic Plasma Source in Jupiter's Magnetosphere II. Near-Io Distribution" will be similar to results presented here but will adopt the new and more accurate neutral source rates noted in Section 3.1. For the O and S isotropic source velocity distributions adopted above, the spatial nature of the Iogenic plasma source has been calculated in three dimensions and collected within spatial grid boxes contained within two different volumes centered around Io's instantaneous location. The linear dimension of the smaller volume about Io is $\pm 1.05 \times 10^4$ km (or ± 5.785 R_{Io}) and is composed of grid boxes with a finer spatial resolution of 600 km (or 0.331 R_{Io}). This volume is comparable to the volume of Io's Lagrange sphere, which has a radius of 5.85 R_{Io}. Along Io's orbit, this smaller volume is equivalent to a longitude angular interval of only $\pm 1.425^\circ$ about the satellite. The linear dimension of the larger volume about Io is $\pm 4.375 \times 10^4$ km (or ± 24.1 R_{Io}) and is composed of grid boxes with a coarser spatial resolution of 2500 km (or 1.377 R_{Io}). This larger scale is important to investigate asymmetries that occur in the Iogenic plasma source because of spatial gradients in the plasma torus that exist near Io's orbit. Along Io's orbit, this linear dimension of this larger volume is equivalent to a longitude angular interval of $\pm 11.889^\circ$ about the satellite.

3.3.1 Instantaneous Source Rates: Near-Io Scale

For the atomic oxygen source, the model calculation of the instantaneous ion pickup rates for electron impact and charge exchange is shown, respectively, in Figures 1a and 1b for a two-dimensional slice in a plane that contains Io and that is perpendicular to the Jupiter-Io outward radial coordinate. In Figure 1 at distances from Io larger than the Lagrange sphere, both the electron impact and charge exchange rates exhibit a north-south asymmetry, as expected. The larger rates below Io are created by the larger electron density in the plasma torus experienced by neutrals that are south of Io and hence closer to the plasma torus centrifugal equator. A longitudinal asymmetry in the downstream direction would also be expected if a description for the Io plasma wake had been included in the model calculation.

Because of the steep radial gradient in the plasma torus near Io's orbit, the Iogenic plasma source will also exhibit a radial asymmetry. This radial asymmetry is exhibited in the profile

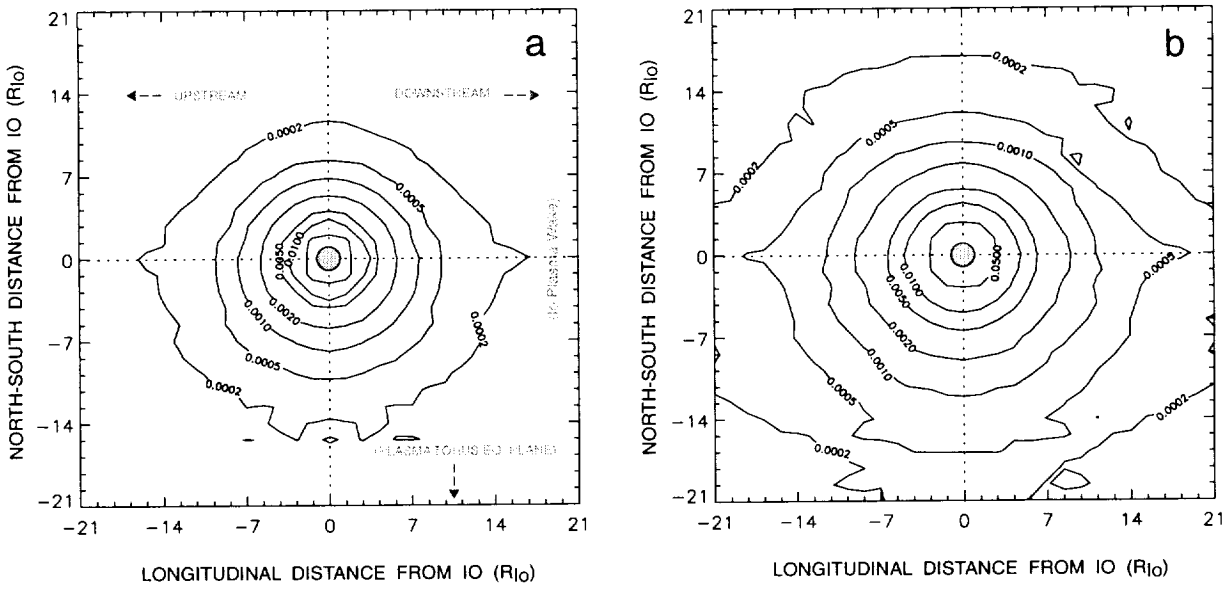

Figure 1. Iogenic Plasma Source Rates for Atomic Oxygen. In a plane through Io and perpendicular to the Jupiter-Io outward radial coordinate, the two-dimensional spatial structure of the ion pickup rate (ions cm^{-3} s^{-1}) that is produced by atomic oxygen is shown in (a) for electron impact ionization and in (b) for charge exchange reactions. Io's location and size are shown by the shaded disk. In the model calculation, an incomplete collisional cascade source of 3.2 x 10^{27} oxygen atoms s^{-1} was assumed at Io's exobase. The ion pickup rates were collected in coarser grid boxes with a spatial resolution of 2500 km.

calculated along the Jovicentric radial coordinate through Io (i.e. perpendicular to the plane in Figure 1) and is shown, respectively, for both atomic oxygen and sulfur in Figures 2a and 2b. Beyond the Lagrange sphere distance, all the profiles inside of Io's orbit can be seen to decrease more rapidly than the profiles outside of Io's orbit because of the steep gradient in the electron density and temperature in the plasma torus near Io's orbit. For atomic oxygen in Figures 1a, 1b, and 2a, the charge exchange rate can be seen to be consistently larger (~3 or greater) than the electron impact ionization rate (EI). In contrast, for atomic sulfur in Figure 2b the electron impact ionization rate (EI) can be seen to be larger (~1.6) than the charge exchange rate outside of Io's orbit and comparable to the charge exchange rate inside of Io's orbit where the electron temperature decreases. This difference in behavior occurs primarily because of the larger ionization potential for atomic oxygen (13.62 eV) as compared to atomic sulfur (10.36 eV). Within Io's Lagrange sphere in Figures 1 and 2, the Iogenic plasma source rates are essentially symmetric about Io. For the finer grid boxes with a resolution of 600 km, an improved model

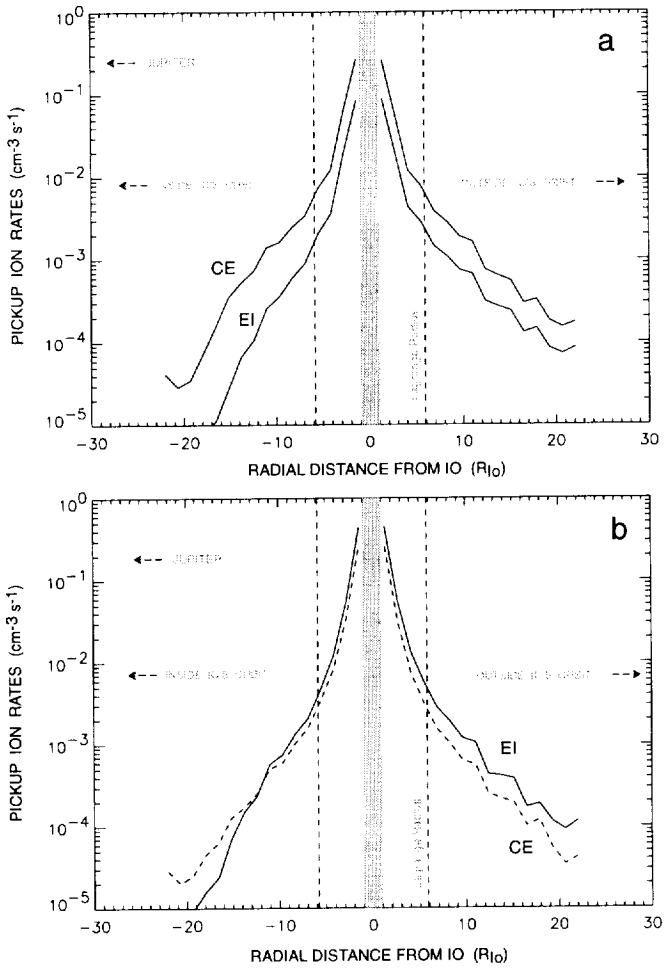

Figure 2. Iogenic Plasma Source Rates for Atomic Oxygen and Sulfur. Calculated radial profiles for the ion pickup rates (ions cm^{-3} s^{-1}) near Io for electron impact ionization (EI) and for charge exchange (CE) are shown in (a) for the atomic oxygen source and in (b) for the atomic sulfur source. The location of Io is shown by the shaded area and that of the Lagrange sphere by the vertical dashed lines. An incomplete collisional cascade source at Io's exobase of 3.2 x 10^{27} atoms s^{-1} and 1.6 x 10^{27} atoms s^{-1} was assumed, respectively, for oxygen and sulfur. The pickup rates were collected in the coarser grid boxes with a spatial resolution of 2500 km.

calculation of this spatial gradient within Io's Lagrange sphere is presented in Figures 3a and 3b for the same calculation shown in Figures 2a and 2b. From Figure 3, the maximum instantaneous CE rate near Io's nominal exobase radius of 2600 km is for atomic oxygen about 0.7 cm^{-3} s^{-1} and 2.1 cm^{-3} s^{-1} (for a ratio of 1 to 3) and for atomic sulfur about 1.8 cm^{-3} s^{-1} and 1.1 cm^{-3} s^{-1} (for a ratio of 1.6 to 1). The combined oxygen and sulfur maximum pickup EI and CE

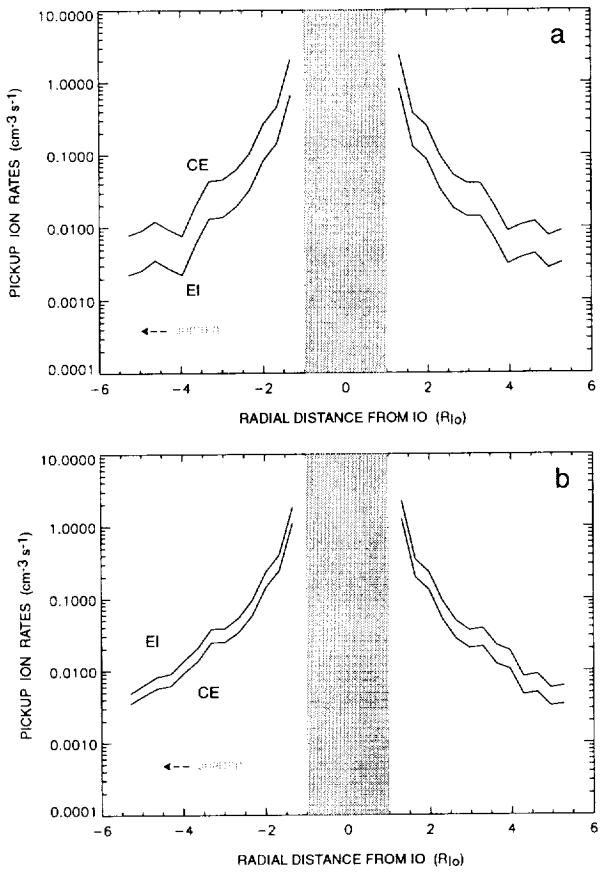

Figure 3. Iogenic Plasma Source Rates for Atomic Oxygen and Sulfur. Same figure caption as for Fig. 2 except that there are no vertical lines for the Lagrange sphere and the pickup rates were collected in the finer grid boxes with a spatial resolution of 600 km.

rates near the exobase are then, respectively, about 2.9 cm^{-3} s^{-1} and 2.8 cm^{-3} s^{-1}, and are essentially the same. The total maximum instantaneous pickup rate is then 5.7 cm^{-3} s^{-1} for the nominal source rates assumed here and for this location of Io, which is significantly north of the plasma torus centrifugal plane. For the new atomic source rate noted above that are ~4.3 times larger, the total instantaneous pickup rate near the exobase would increases to ~25 cm^{-3} s^{-1}, and for a finer grid resolution and convergence of the plasma flow lines (not included here), the local volumetric rate will increase likely by a factor of several and hence may approach ~100 cm^{-3} s^{-1}. This is a significant volumetric source rate at the exobase. It is beginning to approach the generic average source rate value of ~500 to 1000 cm^{-3} s^{-1} that may occur in the Inner Region of the denser atmosphere at and below Io's exobase, as simply calculated from a nominal volume

integrated Iogenic plasma source of ~1 x 10^{28} s^{-1} and an atmospheric volume near Io of ~1-2 x 10^{25} cm^3 for a spherical atmospheric shell of 200-400 km thickness.

3.3.2 Ion Pickup Density: Near-Io Scale

The ion pickup density anywhere in the collection volume about Io can be determined from the instantaneous ion pickup production rate. The ion pickup density is obtained by integrating the ion pickup production rate along a longitudinal tube (parallel to the streamlines) from far upstream to the desired point downstream (see illustration in Figure 4) and dividing this integral by the cross-sectional area of the tube and by the local corotational velocity. This

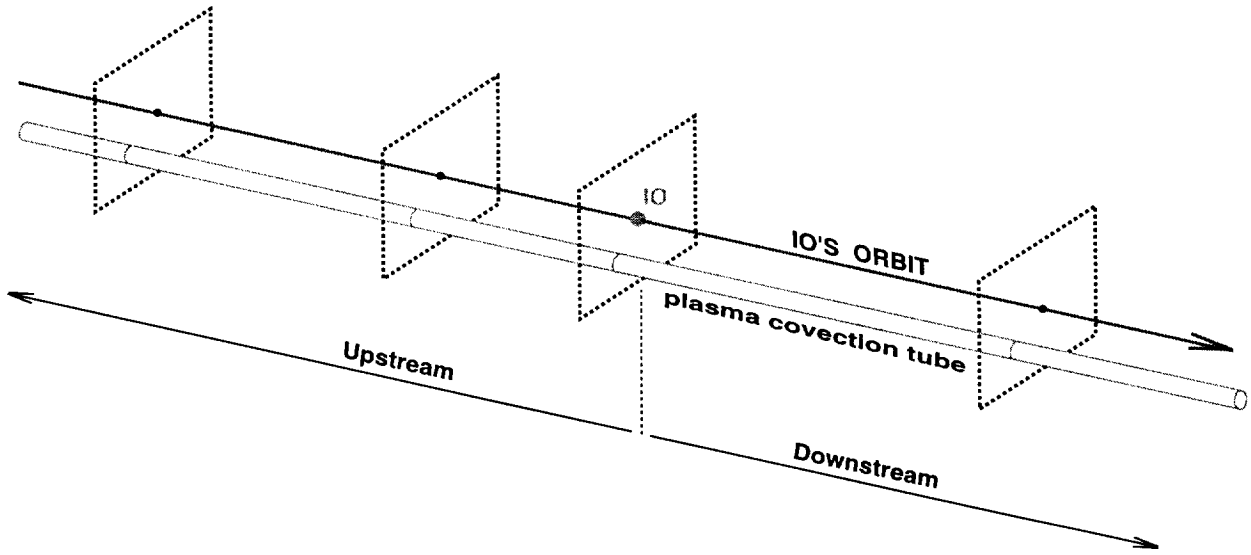

Figure 4. Plasma Convection Tube for Determination of the Ion Pickup Density. The location of Io and several planes perpendicular to Io's orbital motion are shown in relation to a plasma convection tube that extends in the upstream to downstream direction relative to the satellite's location.

integration can be expressed alternatively in terms of the time integral of the motion of the ions along the tube:

$$n_{pickup} = \int_{tube} P_{ion}\, dt\ .$$

Assuming curved streamlines that do not depart from the corotational direction, these integrations have been performed using the larger volume about Io collected with the coarser grid resolution of 2500 km. The ion pickup density is shown in Figure 5 for four selected slices in this volume element that are perpendicular to the corotational direction. In Figure 5a, the low

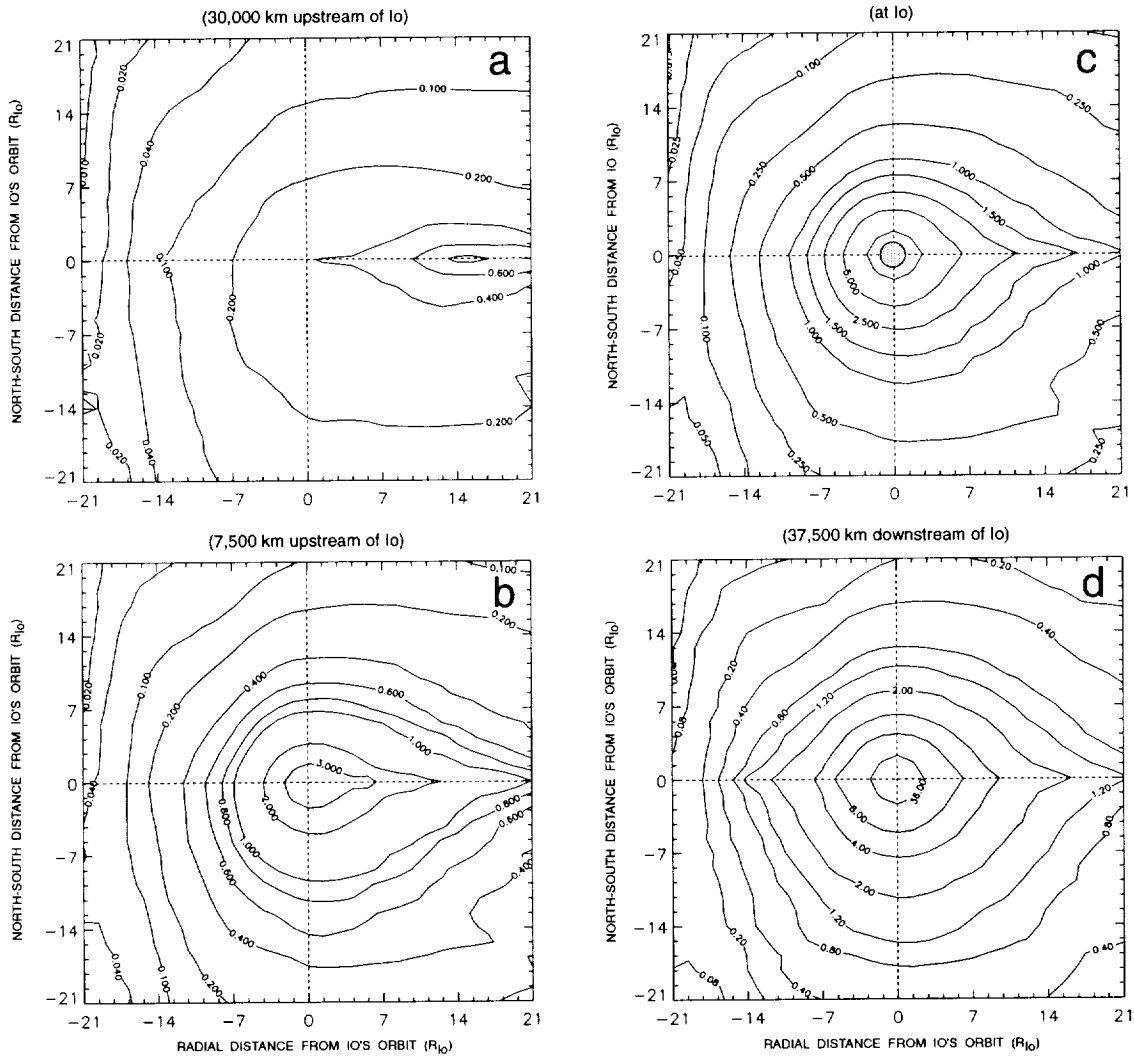

Figure 5. Total Iogenic Pickup Number Density for Atomic Oxygen and Sulfur. In a plane perpendicular to the undisturbed corotational direction, calculated profiles for the ion pickup number density (ions cm^{-3}) are shown in (a) 30,000 km upstream Io, in (b) 7,500 km upstream of Io, in (c) at Io, and (d) 37500 km downstream of Io. The location of Io's orbit is at the intersection of the two dashed lines. Io's location and size is indicated by the shaded circle. An incomplete collisional cascade source at Io's exobase of 3.2×10^{27} atoms s^{-1} and 1.6×10^{27} atoms s^{-1} was assumed, respectively, for oxygen and sulfur. The pickup rates were collected in the coarser grid boxes with a spatial resolution of 2500 km. The inner contour in (c) is 20 cm^{-3}.

ion pickup density located 30,000 km upstream of Io can be seen to be asymmetric located about Io's orbit with a peak occurring at larger radial distances than Io (positive radial values). This pattern occurs primarily because of orbital dynamics that causes the higher-speed neutrals to trail Io at radial distances larger than Io's orbit. In Figure 5b, the ion pickup density located 7,500 km upstream of Io can be seen to be larger and more symmetric about Io's orbit but still exhibits some of the radial asymmetry in Figure 5a because of the contributions of the upstream ions to the downstream location. In Figure 5c, the ion pickup density located in a plane containing Io can be seen to be significantly larger and more nearly symmetric about the satellite. In Figure 5d, the ion pickup density located 37,500 km downstream of Io can be seen to be even larger and is now fairly symmetric about Io's orbit. This more radially symmetric downstream behavior occurs because of the additional source of pickup ions created inside of Io's orbit by lower-speed neutrals that, because of orbital dynamics, lead Io and are located radially within Io's orbit. For the nominal source rate assumed, the ion pickup density near Io's exobase is larger than 20 cm^{-3} (the inner contour). For a more realistic source that is ~4.3 times larger and for a much smaller grid box resolution near Io which should increase the local density by an additional factor of ~5-10 the ion pickup density near the exobase should then be ~ 400-800 cm^{-3}, which is a significant fraction of the nominal undisturbed upstream ion density of ~2000 cm^{-3}. These estimates for the ion pickup density near the satellite can be improved by the inclusion of a more accurate description for the streamlines near Io and by the inclusion of a description for the Io plasma wake in the model calculation of the Iogenic plasma source.

IV. Summary of Related RCM-J Studies

New calculations using the Rice Convection Model for Jupiter (RCM-J) incorporating the effect of a electromagnetic disturbance at Io to represent a localized plasma source were performed and reported at the Fall 2000 AGU meeting (Spiro et al. 2000). These are the first calculations that address the question: How does a localized plasma source influence the transport convection cells in the Io plasma torus? In these new simulations, the following simplifying assumptions were made (although are not required by the model): (1) spin-allowed dipole magnetic field, (2) uniform conductivity in Jupiter's ionosphere, (3) cold torus plasma ($kT << m\Omega^2 r^2 / 2$), and (4) Coriolis force neglected.

The moving localized Iogenic plasma source has two major effects: (1) mass loading of flux tubes intersecting the source region, and (2) associated pickup currents, which close in the Jupiter's ionosphere, resulting in deflection of the corotational flow around Io. As a first step and due to numerical problems, the model does not include the Iogenic plasma source self-consistently. The mass is added to a 30° simulation sector every ~13 hours (Io's period in the plasma torus) with a mass addition rate corresponding to 1/12 (30°/360°) of the normal 10^3 kg/s. The pickup current is represented by a 2-D dipole-like current source in the equatorial plane that propagates through the 30° simulation sector at ~57 km/s (Io's orbital speed with respect to the corotating frame) once every ~13 hrs. The size and strength of this dipole current source corresponds to complete shielding of the corotational flow from a circular radius of one-fourth of a Jupiter radii (~ 10 Io radii), which is physically too large but is a starting point for these initial calculations. For simplicity, the radial outflow of the torus is "impounded" by increasing Jupiter's ionospheric conductivity instead of including corotational lag or a ring-current impoundment. To increase grid density, only a 60° longitude sector is numerically simulated.

In the time evolution of the plasma in the 60° longitude sector, tiny ripples are generated by Io's initial passage and because of the interchange instability grow radially outward in finger-like regions of enhanced plasma per magnetic flux with a characteristic wavelength that is approximately the scale size of the initial electric disturbance. At the second passage of Io, the figure-like structures radially beyond Io's orbit continue to move radially outward, but the base of each finger-like structure at Io's orbital location is undercut and skewed in the direction of Io's motion relative to the outward radial motion of that finger and produces finer and finer spatial structures in this region. The plasma inside of Io orbit is relatively undisturbed by the passage of Io. Mass added from the second passage of Io moves into the fingers formed in the first passage of Io. A similar process occurs on the third passage of Io, with the fingers now much longer in their radial extent.

The inclusion of an Io plasma source makes the physical situation very complicated. The simulations, although very interesting at this stage of development, are not sophisticated enough yet to produce the details correctly. Some of the general features that may be realistic are: (1) the combined effect of the Io-associated pickup current and the interchange-related plasma

fingers generate intricate fine structure in the outer part of the main torus near Io's orbit, (2) structure keeps getting finer and finer as Io traverses the modeled region repeatedly, where in the real system the fine structure presumably diffuses away when it becomes too fine, (3) the inner edge of the torus, which is interchange stable, does not develop the extreme fine structure, and (4) each time Io comes around again, new plasma injected into the plasma torus moves outward following the path of the pre-existing fingers. Additional calculations (Goldstein et al. 2001) including the velocity shear imposed by the corotational lag profiles of the plasma torus near Io's orbit observed by Brown (1994) were presented at the meeting "Jupiter: Planet, Satellites and Magnetosphere" held in Boulder, Colorado during June 25-30, 2001. The velocity shear significantly alters the development of the radial fingers, producing increasingly complex and increasing fine-scale structures down to the smallest scale permitted by the numerical RCM-J simulations. Future improvements in the RCM-J include finding a systematic way of diffusing the fine structure, including impoundment by corotational lag and/or ring current, and having longer simulation times to see if there is an asymptotic behavior for the transport structure.

REFERENCES

Brown, M.E. (1994) Observations of Mass Loading in the Io Plasma Torus, *Geophys. Res. Letts. 21*, 847-850.

Delamere, P.A., W.H. Smyth and M.L. Marconi (2001) Transport Studies of the Radial and Longitudinal Structure in the Plasma Torus, paper presented at the meeting Jupiter: Planet, satellites and Magnetosphere, Boulder Colorado, June 25-30.

Goldstein, J.W., T.W. Hill, R.W. Spiro, and R.A. Wolf (2001) Fine Structure of the Plasma Torus Produced by the Centrifugal Interchange Instability, paper presented at the meeting Jupiter: Planet, satellites and Magnetosphere, Boulder Colorado, June 25-30.

Hill T. W. and D.H. Pontius (1998) Plasma Injection near Io, *J. Geophys. Res. 103*, 19,879-19,885.

Marconi, M.L. and W.H. Smyth (1996) Io Plasma Torus: Nature of the Iogenic Plasma Source, *BAAS 28*, 1154-1155.

Pontius, D.H., R.A. Wolf, T.W. Hill, R.W. Spiro, Y.S. Yang, and W.H. Smyth (1998) Velocity Shear Impoundment of the Io Plasma Torus, *J. Geophys. Res. 103*, 19,935-19,946.

Saur, J., F.M. Neubauer, D.F. Strobel and M.E. Summers (1999) Three-Dimensional Plasma Simulations of Io's Interaction with the Io Plasma Torus: Asymmetric Plasma Flow, *J. Geophys. Res. 104*, 25,105-25,126.

Smyth, W.H. (1992) Neutral Cloud Distribution in the Jovian System, *Adv. in Space Res. 12*, 337-346.

Smyth, W. H. and M. R. Combi (1997) Io's sodium exosphere and spatially extended cloud: A consistent flux speed distribution, *Icarus 126*, 58-77.

Smyth, W.H. and M.L. Marconi (1998) An Explanation for the East-West Asymmetry of the Io Plasma Torus, *J. Geophys. Res. 103*, 9091-9100.

Smyth, W.H. and M.L. Marconi (2000) Io's Oxygen Source: Determination from Ground-based Observations and Implications for the Plasma Torus, *J. Geophys. Res. 105*, 7783-7792.

Smyth, W.H. and M.L. Marconi (2001a) Nature of the Iogenic Plasma Source in Jupiter's Magnetosphere I. Circumplanetary Distribution, preprint in appendix of report.

Smyth, W.H. and M.L. Marconi (2001b) Nature of the Iogenic Plasma Source in Jupiter's Magnetosphere II. Near-Io Distribution, paper in preparation.

Spiro, R.W., R.A. Wolf, T.W. Hill, and J. Goldstein (2000) Effect of a Localized Io Plasma Source on Convection of Torus Plasma, *Eos Trans. AGU 81* (48), Fall Meet. Suppl., Abstract SM61C-08.

Yang, Y.S. (1992) Numerical Simulations of the Jovian-Torus-Driven Plasma Transport, Ph.D. thesis, Rice University, Houston, Texas.

Yang, Y.S., R.A. Wolf, R.W. Spiro, and A.J. Dessler (1992) Numerical Simulation of Plasma Transport Driven by the Io Torus, *Geophys. Res. Lett. 19*, 957-960.

Yang, Y.S., R.A. Wolf, R.W. Spiro, and A. J. Dessler (1994) Numerical Simulation of Torus-Driven Plasma Transport in the Jovian Magnetosphere, *J. Geophys. Res. 99*, 8755-8770.

Appendix:

Nature of the Iogenic Plasma Source in Jupiter's Magnetosphere I.

Circumplanetary Distribution

Nature of the Iogenic Plasma Source in Jupiter's Magnetosphere I. Circumplanetary Distribution

William H. Smyth[1]

and

M.L. Marconi[2]

[1]Atmospheric and Environmental Research, Inc., 131 Hartwell Avenue, Lexington, MA 02421
[2]Fresh Pond Research Institute, 64 Fairfield Street, Cambridge, MA 02140

Abstract

Three-dimensional calculations are presented for the circumplanetary nature of the Iogenic plasma source (pickup ions produced by electron and charge exchange processes in the plasma torus) created by O and S gases located above Io's exobase in its corona and escaping extended neutral clouds (designated as the "Outer Region"). These calculations are undertaken using neutral cloud models for O and S with realistic incomplete collisional cascade source velocity distributions at Io's exobase and realistic spacetime loss processes in the plasma torus. Two-dimensional distributions produced by integrating the three dimensional information along the magnetic field lines are presented for the pickup ion rates, the mass loading rates, the pickup conductivity, the pickup radial current, and the net-energy loading rate. On the circumplanetary spatial scale, the instantaneous Iogenic plasma source is highly peaked about Io's position on its orbit around Jupiter. The degree of orbital asymmetry and its physical origin are discussed and overall spatially integrated rates are presented. The relative importance of the Iogenic plasma source created by the Outer Region and the Inner Region (region below Io's exobase) is estimated and implications are discussed.

1. INTRODUCTION

Jupiter's magnetosphere is dominated by heavy-ion plasma (O^+, O^{++}, S^+, S^{++}, S^{+++}) and has its largest density in the Io plasma torus. The plasma torus is located well within the inner magnetosphere and is organized about (and extends more radially outward of) Io's orbit, which has a radius of 5.9 Jupiter radii (R_J). The heavy-ion plasma is supplied by the loss of neutrals from Io, which has an atmosphere composed primarily of SO_2 and, to a lesser extent, its detected chemically dissociated products (SO, O, S) and trace species (Na, K, Cl). By the Iogenic plasma source, we mean the rate of supply of ions, mass, and energy to the plasma torus created by neutrals from Io. Although the direct loss of ions from Io's atmosphere and ionosphere may involve photoionization, the Iogenic plasma source is created primarily through the direct and more rapid plasma–neutral interactions of electron impact ionization and charge exchange that create new pickup ions for the plasma torus. Understanding the three-dimensional nature of the Iogenic plasma source is highly relevant to a large number of studies for the Io-Jupiter system including the structure and outward transport of the plasma torus and the electrodynamic interactions between the plasma torus, Io, and Jupiter. The heavy-ion plasma supplied to the plasma torus, for example, forms interesting radial structures, as well as System III longitude and dawn-dusk asymmetries, and is ultimately lost by outward radial transport down the tail of the magnetosphere. The creation of the Iogenic plasma source from neutrals from Io can be divided into two spatial regions. First, there is a very spatially confined and denser "Inner Region" below Io's exobase where pickup (i.e., both electron impact ionization and charge exchange) ions are created and also where Pedersen and Hall conductivities become important in the collisionally bound atmosphere and ionosphere. Second, there is a spatially extended and much less dense "Outer Region" above the exobase in the bound corona and in the more distant escaping neutral clouds where pickup ions are also created.

The formation of the Iogenic plasma source in the Inner Region is very complex and involves the solution of a detailed three-dimensional treatment of the nature of the coupling between Io's atmosphere and its electromagnetic interaction in the magnetosphere. Significant efforts to solve this problem have been made in the last few years, but much remains to be accomplished. The two-fluid model approach of Saur et al. (1999) explicitly concentrated on this Inner Region with the primary purpose of solving the electrodynamic problem for a fixed

(unchanging) spherically-symmetric description of the atmosphere. In the one-fluid MHD model approach (Linker et al. 1998; Combi et al. 1998; Kabin et al. 2001), the Inner Region and part of the near-Io Outer Region are represented in a less detailed fashion by including an empirical spatial description for the neutral density in Io's corona (and more recently in the atmosphere) to generate local pickup ions. The Inner Region is also partially represented in the MHD approach by the specification of inner boundary conditions, which may be used, for example, to simulate a "leaky ionosphere". In contrast to the electrodynamic studies for the Inner Region, two-dimensional hydrodynamic studies for the structure, composition and dynamics of Io's atmosphere have been undertaken where the important effects of plasma interactions on shaping the atmosphere have been included in simplified manners (Wong and Smyth 2000; Smyth et al. 2001).

The formation of the Iogenic plasma source in the Outer Region is somewhat less complex and can be calculated in three dimensions using neutral cloud models, which have been developed over the past two decades (see Section II). These numerical models describe the spatial distribution of Io's neutrals above its exobase and their plasma interactions both in the near-Io space of the corona and in the more distant circumplanetary space. Using this approach, the general spatial nature of the Iogenic plasma source for the Outer Region was deduced by Marconi and Smyth (1996). They argued that the neutral clouds of atoms (or molecules), many times mistakenly pictured as being somewhat evenly distributed about Io's circumplanetary orbit, should be primarily spatially concentrated in the general vicinity of Io. This must occur physically because the typical lifetimes (~1 to 20 hrs) for Io neutrals (H, O, S, SO, SO_2) in the plasma torus [due to electron impact ionization (or dissociation) and/or charge exchange reactions] are short compared to the characteristic time to form a complete toroidal cloud about Jupiter at Io's orbit. The destruction of the neutral clouds in the torus should hence produce a spatially extended Iogenic plasma source both upstream and downstream of Io that is highly peaked at the satellite's location.

The Iogenic plasma sources for the Inner Region and Outer Region are coupled in interesting ways through various physical processes involving the corotating plasma torus and neutrals in the Inner Region. The source velocity distribution of neutrals at Io's exobase for the

Outer Region is created in the Inner Region. This source velocity distribution is composed of relatively slow speed neutrals (several km s^{-1}, comparable or less than the Io's surface escape speed of 2.56 km s^{-1}) produced primarily by ion-neutral sputtering processes (and quasi-collisional thermalization processes) and fast neutrals (10's to perhaps 100 km s^{-1}) created by charge exchange processes in Io's local atmosphere. The slow-speed neutrals of the source velocity distribution are important dynamically in determining how the neutrals are distributed in Io's corona and in the circumplanetary space near Io's orbit and consequentially how they contribute in spatial distribution and strength to the Iogenic Plasma Source for the Outer Region. The high-speed neutrals of the source velocity distribution, although observable for some species in the Outer Region, contribute very little to the Iogenic plasma source in the Outer Region but are thought to be a major contributor to the Iogenic plasma source in the Inner Region. Hence, the study of the rates of energization and escape of neutrals from Io has been used as a direct probe to the nature and strength of the local magnetospheric interaction and the Iogenic plasma source in the Inner Region (Smyth 1998; Smyth and Marconi 2000). The Iogenic source rates from the two regions are thought to be comparable (see Section IV). Understanding the relative rates of the Iogenic plasma source in the Inner and Outer Regions is particularly important in understanding the structure and energy budget of the plasma torus. The primary density peak in the plasma torus, the so-called plasma "ribbon", for example, is now thought to be formed by the Iogenic plasma source created in the Inner Region (Smyth and Marconi 1998a; Hill and Pontius 1998; Delamere et al. 2001).

In this paper, the calculations and spatial studies on a circumplanetary scale for the Iogenic plasma source created by for atomic oxygen and sulfur in the Outer Region are undertaken. In a companion paper (Smyth and Marconi 2001), parallel spatial studies of the same Iogenic plasma source on a near-Io scale are presented. The model adopted to calculate the Iogenic plasma source in the Outer Region is discussed in Section II. In Section III, the model calculations for the circumplanetary distribution of the neutral O and S, the pickup ion rates, the mass loading rates, the pickup conductivity, and the pickup radial current are presented. The general spacetime nature of the of the Iogenic plasma source is also discussed. In Section IV, the model results for the Outer Region are discussed and compared with estimates for the Inner Region. A Summary is given in Section V.

2. MODEL FOR THE IOGENIC PLASMA SOURCE

2.1 Neutral Cloud Model

Three-dimensional calculations for the Iogenic plasma source are performed using the neutral cloud model of Smyth and Combi (1988a,b) for satellite corona and extended atmospheres. This model, including various refinements, has been applied over the last 25 years to studying Io's Na cloud (Smyth and McElroy 1977, 1978; Smyth 1979, 1983; Pilcher et al. 1984; Smyth and Combi 1987, 1988b, 1991; Smyth 1992; Smyth and Combi 1997), K cloud (Smyth 1992), O cloud (Smyth and Shemansky 1983; Smyth 1992; Scherb and Smyth 1993; Smyth and Marconi 2000), S cloud (Smyth 1992), and SO and SO_2 clouds (Scherb and Smyth 1993; Smyth and Marconi 1998b) as well as the plasma torus and its interactions with Io (Pilcher et al. 1984; Smyth and Combi 1987; Smyth 1992, 1998; Smyth and Marconi 1998a, 2000; Delamere et al. 2001). The neutral cloud model calculates only the contributions to the Iogenic plasma source created by gases above Io's exobase and hence only in the Outer Region. In this paper, the Outer Region contributions will be limited to those produced by Io's O and S neutral clouds. In brief, the neutral cloud model calculates a large number of three-dimensional neutral particle trajectories by solving the restricted three-body equations of motion, that include the satellite and planetary masses, and, if required, solar radiation acceleration. Appropriate physically weighted information is computed along the trajectories for each time-step to determine the gas density, electron impact ionization and charge exchange rates, and various chemical production rates, which may be velocity as well as spacetime dependent (see Smyth and Combi 1988a,b for the mathematical formulation and more detailed discussions). By following the time history of information along the neutral trajectories, the model calculates the instantaneous neutral gas density and consequently the Iogenic plasma source (the instantaneous ionization and charge exchange rates) that are produced for gas source conditions specified on the exobase of Io moving on its orbit about Jupiter.

The three-dimensional description of the plasma torus adopted in the neutral cloud model is based upon the Voyager 1 plasma properties near western elongation for an offset-tilted dipole magnetic field and includes an inherent System III longitude asymmetry and an east-west (i.e., local time) asymmetry produced by the presence of an east-west electric field. The inherent

System III longitude asymmetry located in the so-called "active sector" (~200-300° System III longitude) has a spatial dependence based upon measurements by Morgan (1985a,b) and an assumed maximum peak electron density that is a factor of two larger than the normal peak plasma torus density outside of the active sector. For the east-west electric field, a nominal value is assumed where ε=0.025 (the ratio of the east-west electric field to the corotational electric field). These Iogenic plasma source rates calculated here hence include the inherently space-time dependent lifetime processes created in the corotating Io plasma torus (1) because of its oscillatory System III latitudinal motion (~$\pm$0.75 R_J) caused by the ~7° tilt between the plasma torus centrifugal equator plane and Io's orbital plane and (2) because of its Jovicentric radial motions (~0.55 R_J) compositely caused in local time by the east west electric field and in System III longitude by the effective dipole-offset of the planetary magnetic field.

2.2 O and S Lifetimes

The lifetime of oxygen and sulfur atoms in the plasma torus is determined by electron impact and charge exchange processes. The reactions and relative importance of these different lifetime processes included in the models are summarized in Table 1 for nominal plasma properties at Io's radial distance in the plasma torus centrifugal equator plane at western elongation (dusk ansa). The charge exchange cross sections adopted in the neutral oxygen and sulfur cloud models are those given by McGrath and Johnson (1989) with refinements provided by R.E. Johnson (personal communication, 1989). At Io's location, charge exchange is seen to dominate over electron impact ionization for atomic oxygen while the reverse is true for atomic sulfur, which has a lower ionization potential. As noted above, all these processes are inherently space-time dependent, and the charge exchange rate is also velocity dependent due to the relative motion of the inhomogeneous plasma torus and the atom trajectories. The relative importance and absolute lifetime s of processes in Table 1 will thus vary in the plasma torus and depend upon local time and the radial, System III latitudinal, and System III longitudinal coordinates. As an example, the electron impact (EI), composite charge exchange (CE), and total (EI + CE) lifetimes of atomic oxygen and sulfur are shown, respectively, in Figures 1 and 2 in a plasmacentric radial and latitudinal coordinate plane that is located at western elongation (i.e., for one local time at the dusk ansa) and at a System III longitude of 230° in the active sector.

The motion of Io in the plasmacentric plane at western elongation for all System III longitudes is indicated by the gray oval, and Io's location on the oval for the System III longitude of 230° is shown by the dot. For atomic oxygen, the EI lifetime (Figure 1a) has an inner minimum (~40 hrs) centered on the centrifugal equator near about 5.9 R_J, where the electron density peak occurs, and an outer minimum (~40 hrs) centered on the centrifugal equator at ~7 R_J, produced by the combined effects of a radially outward increasing electron temperature and a decreasing electron density. The CE lifetime (Figure 1b) for atomic oxygen has only one minimum centered on the centrifugal equator at ~5.9 R_J where the ion number densities are largest. The combined behavior produces a total O lifetime (Figure 1c) at western elongation that has a broader minimum (~5.6-7 R_J) with an absolute minimum still determined by CE processes at ~ 6 R_J. For atomic sulfur, the EI lifetime (Figure 2a) is smaller, as expected, and has a similar spatial structure to atomic oxygen with an inner minimums (~7 hrs) and a outer minimum (just below 10 hrs) centered on the centrifugal equator about ~5.9 R_J and 6.8 R_J, respectively. The CE lifetime (Figure 2b) for atomic sulfur has two relative minimums: a first one (just above 10 hrs) centered on the centrifugal equator at about ~5.3 R_J, that is created by a local maximum in the S^+ plasma torus density, and a second one (just below 10 hrs) centered on the centrifugal equator about ~5.8 R_J. The total sulfur lifetime (Figure 2c) hence has a deeper minimum centered at ~5.9 R_J within a broader minimum (~5.6-7 R_J).

2.3 O and S Source Velocity Distributions at Io's Exobase

The source velocity distribution adopted at the exobase for atomic oxygen and sulfur is the isotropic incomplete collisional cascade distribution determined for sodium by Smyth and Combi (1997). This source distribution peaks at 0.5 km/s, well below the exobase escape speed of ~2 km/s, and extends in the velocity tail to many tens of km/s. This source distribution represents the composite effects of ion sputtering, including heating of the atmosphere. The distribution is denoted "incomplete" because the asymptotic tail power-law behavior of $E^{-4/3}$, where E is the kinetic energy of a neutral, is overpopulated relative to a complete collisional cascade distribution with an asymptotic power-law behavior of E^{-2}. This overpopulation is thought to occur because of the lack of the completion in Io's atmosphere (where escape occurs at the top) of the collision cascade process that moves energy from the velocity tail to the lower-velocity core of the distribution. The incomplete collisional cascade flux distribution

$\phi(v;\alpha, v_b, v_M)$ expressed in terms of the neutral speed, v, is discussed in detail by Smyth and Combi (1988b, in Appendix D) and corresponds to an asymptotic tail power-law behavior given by $E^{-(\alpha-1)}$ and has a peak (most probable) speed of v_m that is related nonlinearly to the velocity parameters v_b and v_M. The core of the source distribution at $v=v_m$ provides an effective parameter to characterize at Io's exobase the composite effects of the complex atmospheric heating processes that occur below the exobase. For the incomplete collisional cascade process, this source distribution should also apply as a first approximation to atomic oxygen and sulfur since sodium is a trace species.

For a set of sodium corona and neutral cloud observations for Io, the incomplete collisional cascade distribution was determined to be essentially isotropic at the satellite exobase with a peak at v_m= 0.5 km/sec (well below the exobase escape speed of ~2 km/sec) and a tail characterized by α=7/3 that extends to many 10's of km/sec [see Smyth and Combi (1997) for the high sensitivity of the fit]. For these parameter values, this normalized source velocity distribution is shown in Figure 3 and is to be adopted in this paper for O and S. About 62% of the source atoms for this distribution are on non-escape trajectories, while the remaining ~32% escape Io's gravitational grasp (Smyth 1998). The composite processes below the exobase that produce this incomplete cascade distribution are yet to be fully understood from first principles by the solution to a complex problem involving the collisional atmosphere and its interaction with the plasma torus. The source distribution thus provides a significant source of O and S atoms with (1) ballistic trajectories (~62%) that populate only the corona of the satellite, (2) low-speed escape trajectories that dynamically are confined relative near Io's orbit, and (3) higher-speed escape trajectories that quickly move away from Io's orbit and contribute primarily to the neutral cloud at somewhat larger and smaller radial distances. For sodium the source speed distribution is responsible for the creation of the very steep gradient near Io in the spatial distribution of sodium within Io's corona as well as the more gradual gradients in the forward sodium cloud and the trailing sodium cloud (excluding the higher-speed contributions by the directional feature source) near Io's orbit. Higher-velocity neutral source processes in Io's local atmosphere (i.e., direct ejection and charge exchange) that are responsible for creation of the sodium directional feature and the sodium zenocorona are, as would be expected, anisotropic with a preferential direction aligned with the plasma corotational motion (see Smyth and Combi 1997 for overview discussion). For the O and S clouds, these higher-velocity neutral source

processes will also create neutrals that directly escape Io's local atmosphere and, along with direct-ion escape, occur in the "Inner Region". These Inner Region contributions to the Iogenic plasma source are, however, not the subject of this paper.

The incomplete collisional source velocity distribution adopted above for O and S is assumed to be isotropic at an Io's exobase radius of 2600 km and have rates determined in the following manner. The O source rate for this distribution was determined by Smyth and Marconi (2000) using the above Io neutral cloud model from the analysis of two different brightness measurements of the O neutral cloud in 6300 A emission. The O source rates obtained in this manner were 1.27×10^{28} and 1.47×10^{28} atoms s^{-1}, respectively, for the measurements of Brown (1981) and Thomas (1996). In this paper, an intermediate O source rate of 1.38×10^{28} atoms s^{-1} (367 kg s^{-1}) is adopted. Since there are currently no direct determinations of the S source rate, a value of 0.69×10^{28} atoms s^{-1} (367 kg s^{-1}), one-half of the O atom source rate as would be appropriate for a parent SO_2 molecule, is adopted for model calculations in this paper. The total source rate at Io's exobase is then 2.07×10^{28} atoms s^{-1} (734 kg s^{-1}) of which only ~38% of the atoms in the source distribution are energetic enough to escape Io's gravity.

3. MODEL CALCULATIONS

3.1 Circumplanetary Asymmetric Distributions

The total nominal lifetime in Table 1 of O and S atoms in the plasma torus centrifugal plane at Io's orbital distance is ~18 hrs and 9 hrs, respectively. For O and S atom trajectories in the near vicinity of Io's orbit, the lifetimes are variable and can be several times larger, as illustrated in Figures 1 and 2. These O and S lifetimes are, however, short compared to the characteristic time of ~250 hrs to form a complete 360° toroidal cloud about Jupiter for the slow escaping neutrals from Io that populate circumplanetary space near Io's orbit in the source distribution of Figure 3. It then follows that the O and S neutral clouds and their Iogenic plasma source contributions must be highly peaked at Io's instantaneous position and hence highly asymmetric in their spatial distributions about Jupiter. There is a particularly interesting and long-standing question to be addressed regarding the nature of this asymmetric circumplanetary distribution for the Iogenic plasma source. Near Io, the volumetric rates (ions or mass cm^{-3} s^{-1}) will be large but the volume will be relatively small compared to the remaining circumplanetary

volume of space. In this large volume of the remaining circumplanetary space, however, the volumetric rates will be much smaller. The question then arises as to the overall comparison of the total (spatially integrated) rates (ions or mass s^{-1}) as a function of circumplanetary distance from Io (i.e., is a large volumetric rate times a small volume larger or smaller than a small volumetric rate times a large volume?).

Model calculations for several ion-pickup volumetric quantities have hence been undertaken in the proximity of Io's orbit on a complete angular scale and a significant radial scale to study the nature of this circumplanetary behavior. For the model description, lifetime processes, and source velocity distribution and rates discussed in Section 2, the instantaneous ion pickup rates have been calculated in three-dimensions and integrated along the magnetic field lines to produce a two-dimensional distribution in the plasma torus with an angular longitudinal resolution of 5° and a radial resolution of 0.1 R_J in the radial interval from 4 to 10 R_J. These model calculations are performed for Io with a geocentric phase angle of 270° (i.e., western elongation or dusk ansa) and an Io System III magnetic longitude of 230° (where Io is north but approaching the plasma torus centrifugal equator plane with a magnetic off-set tilted dipole L value of 5.88). This location of Io provides a substantial instantaneous Iogenic plasma source since the satellite is in the active sector and also the atom trajectories relatively near Io have a time history and local-time location such that they interact strongly with the plasma torus. In the model calculation presented here, the incomplete collisional cascade distribution is represented by nineteen non-uniformly spaced velocity intervals and their corresponding weights. For each velocity interval, 1298 atom trajectories are ejected uniformly from Io's exobase, providing a total number of orbits per neutral cloud model calculation of 24,662. The lifetime history for each atom trajectory is computed sufficiently far in the past to achieve a steady state description for the neutral cloud and the instantaneous Iogenic plasma rates for Io's location chosen above for the model calculation.

3.2 Distribution of O and S

It is important to understand the spatial distribution about Jupiter of the O and S densities that are shaped by the processes in Table 1 in order to understand the spatial nature of the Iogenic plasma source that they create. The O and S neutral densities have been calculated in

three-dimensions and integrated perpendicular to Io's orbit plane to produce a two-dimensional distribution with a spatial resolution box size of 2 x 10^4 km [~11 Io radii (R_{Io})]. The model calculated O and S neutral column densities viewed perpendicular to Io's orbital plane are given in Figures 4a and 4b, respectively. Both the neutral O and S column density distributions are highly peaked about Io's instantaneous position (small dot at western elongation) and are highly asymmetric in longitude. The O and S atoms are concentrated primarily ahead and inside of Io's orbit (i.e., forward cloud) where the neutral loss rates in the plasma torus are small because of the rapidly radially inward decreasing plasma densities and temperatures. Over a larger circumplanetary volume, ranging from near Jupiter to a bit beyond Io's orbit (and preferentially asymmetrically located behind Io's orbital position), the O and S column densities are a factor of ~50-100 or so times smaller than in the general vicinity of Io. For both the trailing O and S neutral clouds, the column density decreases more rapidly with angular distance from Io than the forward cloud because the trailing cloud gases are primarily located outside of Io's orbit (because of orbital dynamics) where the plasma torus loss processes are continuously operative. On a circumplanetary scale, the column density for atomic oxygen is significantly larger (factor ~5) than for atomic sulfur because of the shorter lifetime of atomic sulfur in the plasma torus and the factor two smaller sulfur source rate. In Figure 4c, the asymmetry of the column density profiles for oxygen and sulfur along the horizontal dashed line are shown in Figures 4a and 4b. For O, the peak column density at Io is ~4 x 10^{13} atoms cm^{-2} compared to ~5 x 10^{11} atoms cm^{-2} diametrically opposite Io on the satellite orbit (dashed circle), a factor of about 80 smaller. For S, the peak column density at Io is ~1.8 x 10^{13} atoms cm^{-2} compared to ~8 x 10^{10} atoms cm^{-2} diametrically opposite Io on the satellite orbit (dashed circle), a factor of about 225 smaller, reflecting the smaller lifetime for S.

3.3 Distribution of the Pickup Ion Rates

The loss processes for the neutrals in Table 1 are the same processes that create the pickup ions for the plasma source and hence determine the Iogenic plasma source for the Outer Region. In discussing pickup ion rates, it is important to differentiate the "new pickup ion rate" from the "net pickup ion rate". All of the reactions in Table 1 for electron impact (EI) ionization and charge exchange (CE) processes create new ions and hence contribute to the "new pickup ion rate". These newly created ions, in the presence of the magnetospheric local electric and

magnetic fields, create pickup currents as they are accelerated to the local plasma corotational speed and are energize gyrationally. All of the EI reactions, but only some of the CE reactions in Table 1, however, create net ions for the plasma torus and hence are able to contribute to the "net pickup ion rate". Symmetric charge exchange reactions (e.g. $S + S^+ \rightarrow S^+ + S$; $O + O^{++} \rightarrow O^{++} + O$) do not contribute to the net pickup ion rate or to the corresponding net-mass pickup ion-loading rate of the plasma torus. Asymmetric charge exchange reactions (e.g. $S + O^+ \rightarrow S^+ + O$; $O + S^+ \rightarrow O^+ + S$) do not contribute to the net pickup ion rate but can contribute either positively or negatively to the net-mass pickup ion-loading rate. Finally, charge transfer reactions (e.g., $O + S^{++} \rightarrow O^+ + S^+$) contribute positively both to the net pickup ion rate and the net-mass pickup ion loading rate. Since the symmetric charge exchange reactions are the dominant CE processes in Table 1, it follows that the CE processes play a much less important role compared to the EI processes in their contributions to net pickup ion rate and to the net-mass pickup ion loading rate. The CE processes, however, provide a strong contribution to the pickup ion conductivity and current and also to the net-energy loading rate for the plasma torus.

The instantaneous new ion pickup rates produced by electron impact (EI) ionization and the set of charge exchange (CE) processes in Table 1 are shown, respectively, for the O neutrals in the Outer Region in Figures 5a and 5b and for the S neutrals in Figures 5d and 5e. One-dimensional profiles for the new pickup ion rates for the EI and CE processes are also shown along an east-west dashed line (i.e., the line through Io and Jupiter) in Figures 5c for O and in Figure 5f for S to better display their circumplanetary asymmetry. For both oxygen and sulfur, the new ion pickup rates are highly peaked about Io (small dot at western elongation). An examination of the nature of the pickup ion distributions near Io at a higher-spatial resolution than considered here is presented in a companion paper (Part II). All of the pickup ion rates in Figure 5 decrease rapidly inside of Io's orbit because the plasma torus densities and temperatures decrease rapidly there with decreasing radius.

A comparison of the new pickup ion rates for EI created by O (in Figure 5a) and S (in Figure 5d) shows that they have almost identical circumplanetary distributions near and inside of Io's orbit. This same morphology occurs because the factor of ~5 larger column density for O than for S (in Figure 4) is compensated by the factor of ~5 times smaller electron ionization lifetime for S than for O. Well outside of Io's orbit, the new pickup ion rate produced by O

becomes larger than that produced by S, since the factor of ~5 enhancement in the O column density is no longer fully compensated by the electron ionization lifetime that, at these larger distances (see Figures 3a and 4a), is now only a factor of ~2 times smaller for S than O. Examination of the one-dimensional profiles peaks in Figures 5c and 5f, which occur at Io and diametrically opposite Io on its orbit, shows that the new pickup ion rate for EI pickup processes in Figures 5a and 5d differ at the two positions by a factor of ~600 for O and ~1000 for S.

For CE processes, the pickup ion rates created by O (Figure 5b) and for S (Figure 5e) are highly peaked in a narrow radial interval occupying angularly incomplete forward and trailing arms that reach out from Io and are located from just outside to just inside of Io's orbit, where the charge exchange lifetimes have their minimum values. In these arms, the new pickup ion rate created by O is larger than for S by a factor ~4, which is caused by the factor of ~5 larger O column density and a slightly smaller S electron charge exchange. At radial distances well outside Io's orbit, the new pickup ion rate for O relative to S becomes even larger (~20) because the S column density decreases more rapidly with Jovicentric distance than the O column density. Examination of Figures 5c and 5f shows that the ratio of the new pickup ion rate at Io to that diametrically opposite Io on its orbit is ~340 for S and ~140 for O.

The spatially integrated new pickup ion rates produced by the EI and CE processes in Figure 5 and also the associated net pickup ion rates are summarized in Table 2. For EI processes, the integrated new pickup rates for O (1.28×10^{27} ions s^{-1}) and S (1.75×10^{27} ions s^{-1}) are comparable, as expected, with the larger rate for the S with the shorter ionization lifetime and hence the larger source rate near Io (see Figures 5c and 5f). For CE processes, the integrated new pickup rate for O (3.47×10^{27} ions s^{-1}) is considerably larger than for S (1.05×10^{27} ions s^{-1}) and reflects the shorter charge exchange lifetime and larger source for O near Io. For O and S combined, the EI (3.03×10^{27} ions s^{-1}) and the CE (4.52×10^{27} ions s^{-1}) contributions are comparable and are ~40 and 60%, respectively, of the overall integrated new pickup ion rate of 7.55×10^{27} ions s^{-1}. The spatially-integrated net pickup ion rate (3.85×10^{27} ions s^{-1}) is about one-half this rate and is created mainly (79%) by an EI contribution (3.03×10^{27} ions s^{-1}) with a smaller (21%) CE contribution (0.82×10^{27} ions s^{-1}).

3.4 Distribution of the Total-Mass and Net-Mass Loading Rates

The instantaneous equivalent (EI + CE) total-mass loading rate ($\dot{M}^{(EI)} + \dot{M}^{(CE)}$) for the Io plasma torus is determined directly from the pickup ion rates for EI and CE processes, denoted here by S_o^{EI} and S_o^{CE} for O and by S_s^{EI} and S_s^{CE} for S, respectively:

$$\dot{M}^{(EI)} = m_o S_o^{EI} + m_s S_s^{EI} \tag{1a}$$

$$\dot{M}^{(CE)} = m_o S_o^{CE} + m_s S_s^{CE} \tag{1b}$$

where m_o and m_s are the mass of an O and S ion, respectively. The instantaneous net-mass loading rates $\dot{M}^{(net)}$ are determined straightforwardly by adding the rate of creation of ion mass for all EI processes and of the net ion mass contributions for all CE processes (see Smyth and Combi 1988a for a more detailed formulation). The circumplanetary distribution of the instantaneous net-mass loading rates and the equivalent total-mass loading rate integrated along the magnetic field line are shown, respectively, in Figures 6 and 7.

The nature of the angular distribution of the net-mass loading rates about Jupiter has been an interesting and open question. Suggestions for the shape of the distribution have ranged from the extremes of an angular distribution that is uniform in a toroidal volume about Jupiter to a distribution that is very highly localized in the immediate vicinity of Io's instantaneous position. The distribution in Figure 6a has the character of an immediate state: the source is both very highly peaked at Io's instantaneous position and also exists at much lower levels all around Jupiter. To quantify this angular variation more succinctly, the two-dimensional distribution in Figure 6a is integrated radially within 5° pie-shaped angular intervals to produce the average angular distribution shown in Figure 6b. Examination of this angular distribution shows that it may be effectively divided into a highly peaked component near Io that is located approximately within ±20° of Io's instantaneous position and a more gradually decreasing component that has a minimum located approximately on the opposite side of Jupiter from Io. The steeper slope, occurring for System III longitudes that are larger than Io, corresponds to the plasma source that is located behind (i.e., upstream) of Io and primarily outside its orbit in the hotter region of the plasma torus. The less steep slope for System III longitudes smaller than Io corresponds to the plasma source that is ahead (downstream) of Io and primarily within (but near) its orbit, where

the neutral loss processes are still rapid enough to contribute significantly to the Iogenic source. The total (EI + CE) pickup ion equivalent mass-loading rate has a similar morphology and is shown in Figures 7a and 7b.

The spatially integrated net-mass loading and total equivalent mass-loading rates for Figures 6 and 7 are, respectively, 154 and 277 kg s^{-1}. In Table 2, these "Outer Region" integrated rates are separated into their contributions from electron impact ionization and charge exchange. The net-mass loading rate of 154 kg s^{-1} is created primarily by electron impact ionization (127 kg s^{-1}) but also has a small contribution from charge exchange processes (27 kg s^{-1}) because of asymmetric charge exchange and charge transfer reactions in Table 1. The net-mass loading rate within the ±20° of the Io peak in Figure 6 is about 109 kg s^{-1} (71% of the spatially integrated rate) with only 45 kg/s (29%) located within the remaining 320° angular interval about Jupiter. The total mass-loading rate within the ±20° of the Io peak in Figure 7 is about 197 kg/s (also 71% of the spatially integrated rate) with only 80 kg/s (29%) located within the remaining 320° angular interval about Jupiter.

3.5 Distribution of the Net-Mass per unit Magnetic Flux Source Rate

One of the volumetric quantities of interest for transport studies in the plasma torus, such as those undertaken with the Rice Convection Model for Jupiter (RCM-J; see, for example, Pontius et al. 1998), is the source rate for the net-mass per unit magnetic flux integrated along the magnetic field, which is denoted by η:

$$\eta = \int \frac{\dot{M}^{(net)}}{B} ds \qquad (2)$$

where B is the local value of the magnetic field, and "ds" is the differential distance element along the magnetic field line. For the combined O and S pickup ion rates discussed above, the two-dimensional spatial distribution for this instantaneous source rate η is shown in Figure 8.

The circumplanetary distribution for the net-mass per unit magnetic flux in Figure 8a is highly peaked at Io's location and is enhanced in both forward and trailing arms near Io's orbit

and in an extended radial region outside Io's orbit and trailing Io's orbital location. Upon comparison with the net-mass distribution in Figure 6a, the distribution in Figure 8a is seen to be skewed by the ~L^3 nature of the factor of 1/B in the definition for η (where B= 1835 nT near Io's orbit) so as to be relatively lower by about a factor of ≤ 2 inside of Io's orbit and to be relatively enhanced by up to a factor of 4 or more outside of Io's orbit. In Figure 8b, the degree of asymmetry of the distribution is shown in a profile taken along the dashed horizontal line in Figure 8a through Io. The maximum value at Io is ~6×10^{-8} kg m^{-2} s^{-1} T^{-1} and is a factor of ~ 600 times larger than the peak diametrically opposite Io on its orbit.

3.6 Distribution of the Pickup Conductivity, Current, and Power

The pickup ion rates produced by the O and S neutrals also produce a pickup conductivity σ_{pu} through the introduction of ion-electron pairs, which are separated on average by their gyration radii at the initial times of their creation (Goertz 1980). The pickup conductivity depends upon all EI and CE processes and is defined by

$$\sigma_{pu} = \frac{\dot{M}^{(EI)} + \dot{M}^{(CE)}}{B^2} . \tag{3}$$

The height-integrated pickup conductivity Σ_{pu} is defined by integrating σ_{pu} along the magnetic field line

$$\Sigma_{pu} = \int \sigma_{pu} ds . \tag{4}$$

In an Io frame with the corotational radial electric field denoted by $\vec{E}$, the pickup conductivity generates a radial pickup current density $\vec{J}_{pu}$ (amps m^{-2}), which is given by

$$\vec{J}_{pu} = \sigma_{pu} \vec{E} . \tag{5}$$

The instantaneous radial pickup current I_{pu}(amps) at a function of radius and System III longitude defined through a surface with a differential area $dA = \ell ds$, where one dimension is along the field-aligned height-integrated direction "s" and the second dimension is along the System III longitude direction with a arc length ℓ corresponding to the adopted circumplanetary grid resolution of 5°, can also be determined from $\vec{J}_{pu}$

$$I_{pu} = \int \left| \vec{J}_{pu} \right| dA \ . \tag{6}$$

The power density P_{pu} (watts m^{-2}) required to produce the new pickup ion rates in Io's reference frame is determined from $\vec{J}_{pu}$ as follows:

$$P_{pu} = \int \vec{J}_{pu} \cdot \vec{E} \, ds = \int \sigma_{pu} \, E^2 ds \tag{7a}$$

and may be written alternatively as

$$P_{pu} = \frac{1}{2} \int (\dot{M}^{(EI)} + \dot{M}^{(CE)}) V_{cor}^2 \, ds + \frac{1}{2} \int (\dot{M}^{(EI)} + \dot{M}^{(CE)}) V_{cor}^2 \, ds \ . \tag{7b}$$

where the local corotational pickup speed V_{cor} is

$$V_{cor} = \left| \vec{V}_{cor} \right| = \left| \frac{\vec{E} \times \vec{B}}{B^2} \right| = \frac{E}{B} \ . \tag{8}$$

The expression (7b) for the power density P_{pu}, which has been divided into two equal parts, has an obvious interpretation. The first half of the power density is the work required by the electric field to accelerate the center-of-mass motion of the pickup ions to the local corotational speed of the plasma torus, while the second half is the power required to energize the gyrational motion of the ions relative to their center-of-mass motion. This center-of-mass motion of the pickup ions is reflected in the expression for the force exerted on the pickup ions

$$\vec{J}_{pu} \times \vec{B} = \sigma_{pu} \, \vec{E} \times \vec{B} = (\dot{M}^{(EI)} + \dot{M}^{(CE)}) \frac{\vec{E} \times \vec{B}}{B^2} = (\dot{M}^{(EI)} + \dot{M}^{(CE)}) \vec{V}_{cor} \ . \tag{9}$$

The gyration power of the new pickup ion energy is the rate of energy at which new ions are created to heat the plasma torus, i.e., the "new pickup ion energy loading rate". It is, however, larger than the "net pickup ion energy loading rate" for the plasma torus since symmetric and asymmetric charge exchange reactions transform old cooler ions of the plasma torus into fast neutrals that rapidly escape from the plasma torus with the energy of the old cooler ions.

The circumplanetary distribution of the height-integrated pickup conductivity Σ_{pu} is shown in Figure 9a. The pickup conductivity Σ_{pu} is seen to be highly peaked at Io's location

and is enhanced in both forward and trailing arms near Io's orbit and in an extended radial region outside Io's orbit and trailing Io's orbital location. Upon comparison with the total-mass distribution in Figure 7a, the distribution in Figure 9a is seen to be heavily skewed by the $\sim L^6$ nature of the factor of B^{-2} in the definition for σ_{pu} so as to decrease more rapidly inside of Io's orbit and to decrease much more slowly outside of Io's orbit. In Figure 9b, the degree of asymmetry of the distribution is shown in a profile taken along the dashed horizontal line in Figure 9a. The maximum value at Io is $\sim 2.5 \times 10^{-3}$ mho and is a factor of ~ 450 times larger than the peak diametrically opposite Io on its orbit.

The circumplanetary distribution of the radial pickup current I_{pu} is shown in Figure 10a. The radial pickup is highly peaked at Io's location and asymmetrically distributed about Jupiter with enhanced forward and trailing arms that extend further outside of Io's orbit near the satellite and become confined very near Io's orbit at much larger angular distances from the satellite. In Figure 10b, the peak current at Io is $\sim 4 \times 10^4$ amps while that at the location opposite Io on its orbit is ~100 amps, an asymmetric factor of 400 smaller.

The circumplanetary distribution of the net-energy loading rate is shown in Figure 11a and is highly peaked at Io and has a morphology in asymmetric angular similar to the radial pickup current in Figure 10a. In Figure 11b, the peak net-energy loading rate at Io is $\sim 6 \times 10^{-4}$ watts m^{-2} as compared to $\sim 1.8 \times 10^{-6}$ watts m^{-2} diametrically opposite Io on the satellite orbit, an asymmetry factor of over 300. The spatially integrated net-energy loading rate for Figure 11a is 1.03×10^{12} watts and is dominated by the contribution from the large peak at Io.

3.7 Spacetime Variability of the Iogenic Plasma Source

To understand the general nature of the space-time variability of the Iogenic plasma source rates (e.g., the net ion-loading rate, net mass-loading rate, equivalent mass loading-rate for momentum loading, and energy-loading rate), it is important to understand the relationship between the instantaneous neutral source rate at Io, the neutral cloud instantaneous accumulation

rate in the circumplanetary space, and the instantaneous loss rates of neutrals in the magnetosphere, the latter of which produces the Iogenic plasma source. The relationship among these three quantities has been derived mathematically using the general "ensemble packet" formalism developed by Smyth and Combi (1988a). The results are presented briefly below.

Consider on Io's exobase a solid angle element $d\Omega$ at the location $\hat{\Omega}$ and atoms ejected from this element with a velocity in the range $\bar{\omega}$ to $\bar{\omega} + d\bar{\omega}$. We denote the neutral source rate (atoms per second) originating with the conditions $(\bar{\omega}, \hat{\Omega})$ at time T by $\phi(\bar{\omega}, \hat{\Omega}, T)\, d\bar{\omega}\, d\Omega$ where $\phi(\bar{\omega}, \hat{\Omega}, T)$ is the flux per unit $d\Omega$ and per unit $d\bar{\omega}$. We denote by $N(\bar{\omega}, \hat{\Omega}, T)\, d\bar{\omega}\, d\Omega$ the number of neutrals at time T along the complete neutral trajectory formed prior to the time T and originating with the conditions $(\bar{\omega}, \hat{\Omega})$. We furthermore denote the neutral cloud instantaneous accumulation rate at time T for atoms originating with the conditions $(\bar{\omega}, \hat{\Omega})$ for past times up to time T by

$$\frac{dN(\bar{\omega}, \hat{\Omega}, T)}{dT}\, d\bar{\omega}\, d\Omega. \tag{10}$$

Finally, we denote by $L(\bar{\omega}, \hat{\Omega}, T)\, d\bar{\omega}\, d\Omega$ the instantaneous neutral cloud loss rate at time T caused by magnetospheric processes for the complete trajectory originating with the conditions $(\bar{\omega}, \hat{\Omega})$. The desired relationship between these three quantities may then be expressed as follows

$$\phi(\bar{\omega}, \hat{\Omega}, T) - \phi^{(exit)}(\bar{\omega}, \hat{\Omega}, T) = \frac{dN(\bar{\omega}, \hat{\Omega}, T)}{dT} + L(\bar{\omega}, \hat{\Omega}, T) \tag{11}$$

where $\phi^{(exit)}(\bar{\omega}, \hat{\Omega}, T)$ is the instantaneous atom flux along the trajectory that is lost from the trajectory because of collision with Io, collision with Jupiter, or that remains undepleted and unchanged on the trajectory having been ejected from Io at times prior to time T.

The equation (11) is a conservation statement at time T for the complete trajectory originating with the conditions $(\bar{\omega}, \hat{\Omega})$. Since it is valid for all neutral trajectories from Io's

exobase, it also follows that it is true for the neutral cloud as a spatially integrated whole by simply integrating over all conditions at the exobase. The left hand side of equation (11) is the instantaneous net flux at time T from Io that is available to either increase the neutral cloud abundance along the entire trajectory or to supply the neutral cloud loss rate caused by the magnetospheric processes. Note that this neutral cloud loss rate may be smaller than the net flux if the abundance of neutrals along the trajectory is increasing or may be larger than the net flux if the abundance of neutrals along the trajectory is decreasing. Hence, the neutral cloud is a reservoir for the neutrals that can increase in abundance when the global loss rate becomes smaller and can decrease in abundance when the global loss rate becomes larger. The time variability in the loss rate is caused by the oscillation of the plasma torus about Io's orbital plane, the System III longitude asymmetries of the plasma torus, and the east-west asymmetries of the plasma torus. Hence, the instantaneous strength of the Iogenic plasma source determined by the neutral cloud loss rate may be larger than the instantaneous net flux at time T from Io if the neutral cloud loss rate is decreasing and conversely may be smaller than the instantaneous net flux at time T from Io if the neutral cloud loss rate is increasing. Hence, it is not the instantaneous net flux at time T from Io that determines the instantaneous strength of the Iogenic plasma source but the complete time history at time T of the neutral cloud.

4. DISCUSSION

4.1 Comparison of Inner and Outer Region Iogenic Sources

Several estimated rates for the spatially integrated Iogenic plasma source are summarized in Table 4. These rates combine in various ways contributions from the Inner Region and the Outer Region and hence can be considered to be approximate estimates for the total Iogenic plasma source. The estimates of Smyth (1992) and Smyth and Marconi (2000) were obtained from neutral exobase source rates for Io determined by modeling the spatial brightness distribution of the neutral clouds and from additional scaling arguments to extend the velocity range to include high-speed charge exchange processes. The estimates of Smyth (1992) used monoenergetic source conditions to describe the slower neutrals at Io's exobase rather than the more accurate description of the incomplete collisional cascade distributions used here and in Smyth and Marconi (2000). Hence, the more recent estimates must be considered to be more

accurate. The estimates of Smyth and Marconi (2000) include rates for the Outer Region, essentially those presented in this paper, and additional estimated rates for the Inner region that are included only for charge exchange processes. The estimates of Bagenal (1997) were obtained from examination of the Galileo PWS electron data (Gurnett et al. 1996) and PLS plasma data (Frank et al. 1996). The rates for Combi et al. (1998), Linker et al. (1998), and Kabin et al. (2001) were obtained from MHD modeling of the Galileo PLS plasma (Frank et al. 1996) and MAG magnetic field data (Kivelson et al. 1996) and are listed for different scenarios, which provided marginal fits for most of the data but failed to reproduce the two local minima in the magnetic field on the wake flanks. Combi et al. (1998), who did not solve for the magnetic field inside of the satellite, considered two different inner boundary conditions [fixed (f) and reflective (r), in Table 4] at an altitude of 150 km to span extreme conditions for the particle and magnetic field interactions with Io and its ionosphere. For the "reflective" boundary conditions, Io and its ionosphere are treated as a perfect conducting impenetrable sphere so that both the magnetic field and plasma flow are reflected. For the "fixed" boundary conditions, the magnetic field and particles can penetrate the ionospheric boundary and are treated at the boundary by setting the fluid velocity to zero, the density to ionospheric values, and fixing the magnetic field so that only a small expected change occurs in its value inside Io's solid body. Linker et al. (1998), who solved for the magnetic field inside of Io, considered the case of an Iogenic plasma source with both a magnetized and non-magnetized Io [labeled, respectively, (m) and (n) in Table 4]. Kabin et al. (2001) added to the earlier treatment of Combi et al. (1998) new pickup ion terms into the equations and included, in addition to a power law description for the neutral density in Io's corona, an exponential scale-height term to describe Io's atmosphere nearer the surface and also a day-night asymmetry in the neutral density distribution.

The estimates of Smyth (1992) and Smyth and Marconi (2000) have a ratio of the charge exchange rate to the net mass-loading rate of ~1.6 and ~3.3, respectively, which is similar to the values of ~1.1, ~1.8, and 3, respectively, for Kabin et al. (2001), Combi et al. (1998), and Linker et al. (1998) but is in striking contrast to the values of Bagenal (1997), who concluded that there was no significant charge exchange rate near Io at the time of the Galileo flyby. Since charge exchange reactions are always operative and physically dominant over electron ionization rates at Io's position in the undisturbed plasma torus, this conclusion is suspect. The conclusion of

Bagenal (1997) can be traced effectively to an arbitrary division of the flux of the "new ionized ions" from the "background ions" in the PLS and PWS measurements. In Table 4, the estimates for the total new pickup ion rate of 5 x 10^{28} ions s^{-1} for the more extreme reflective boundary condition model [labeled (r)] of Combi et al. (1998) is likely too large. This larger source rate was required to supply the same amount of plasma density to the plasma wake region, where in this case both the particles and the magnetic field are highly reflected by the inner boundary and are therefore distributed over a larger spatial volume. The smaller total source rate (n) of Linker et al. (1998) is also likely too small since it was determined for the case of an assumed intrinsic magnetic field for Io, which does not now appear to be supported by MHD modeling of more recent Galileo flyby magnetospheric data (Linker et al. 2001). With these limitations then, the best estimates obtained from Table 4, which represent the combined contributions of the Inner and Outer Regions, are very similar and are in the range ~1.7–2.7 x 10^{28} ions s^{-1} for the total new pickup ion rate and ~600–980 kg s^{-1} for the total mass loading rate.

The estimates of the new mass loading rate for the Iogenic plasma source for the Inner Region determined in this paper and for the combined Inner and Outer Regions obtained from Table 4 are summarized in Table 5. By subtracting these rates, a rough estimate for the new mass loading rate for the Inner Region is therefore ~300 to 700 kg s^{-1} so that the rate for the Inner Region is ~1 to 2.5 larger that for the Outer Region. The Inner Region is, however, highly concentrated in a small volume around Io. In contrast, the primary peak of the Outer Region at Io, which contains ~71% (125 kg s^{-1}) of the new mass loading rate, is located within a large volume with angular dimension of ±20° longitude (i.e., ±81 R_{Io}) about Jupiter. A more detailed description of the spatial distribution of Iogenic plasma source for the Outer Region within this large volume is the subject of the companion paper. Hence volumetrically, the Iogenic plasma source near Io must be dominated by the Inner Region contribution. Similarly, the net energy pickup rate of ~1 x 10^{12} watts calculated for the Outer Region is less than the ~2-5 x 10^{12} watts estimated for the total energy budget of the plasma torus. The Inner Region should thus also be expected to have a comparable or larger contribution, which should balance the energy budget. The asymmetries in the Iogenic plasma sources at Io will therefore be much larger than those presented in Section 3 for the Outer Region source only. Given this perspective, it should not be so surprising that the plasma torus ribbon, the dominant radial density feature in the plasma

torus, is created by the Iogenic plasma source created in the Inner region (Smyth and Marconi 1998a; Hill and Pontius 1998; Delamere et al. 2001) and that the energy budget of the plasma torus is very dependent upon the power ribbon created by this Inner Region source (Smyth and Marconi 2000).

4.2 Additional Iogenic Sources

The Iogenic plasma source calculations presented in Section 3 were only for pickup ions created by O and S gases in the Outer Region. These rates may only be a lower limit if other species (SO_2, SO, O_2, S_2) in Io's atmosphere can also contribute significantly to the Iogenic plasma source in the Outer Region. The abundances of O_2 formed through atmospheric chemistry and S_2 released by volcanoes are both thought to be too small on a global scale to provide a significant source of pickup ions. The most abundant species SO_2 and the next most abundant species SO (~10% of SO_2) in Io's atmosphere are expected to undergo rapid electron impact dissociation in Io's upper atmosphere (Smyth et al. 2001) producing primarily O and S exothermic atomic products. The electron impact production rate for molecular ions is small compared to that for molecular neutral products. Much of the exothermic O and S source rates at the exobase may, however, already effectively be included in the source rates for the Outer Region adopted here, which are calibrated by observations for atomic oxygen. The direct escape of SO_2 and SO from the exobase may, however, provide some spatially extended source of exothermic O and S to the circumplanetary space, although SO is likely to be less important because of its order of magnitude smaller abundance relative to SO_2 in Io's atmosphere. The SO_2 and SO exobase source rates are not well known, and their exothermic O and S energy distributions have not been measured. An SO_2 exobase source rate of 4×10^{27} molecules s^{-1} was given by Smyth and Marconi (1998b) based upon the analysis of ion cyclotron waves for a maximum SO_2^+ density profile determined by Huddleston et al. (1997) and the same incomplete collisional source distribution adopted in this paper for O and S. Hence only ~38 percent of the SO_2 molecules are on escape orbits, providing an SO_2 escape flux of $\sim 1.5 \times 10^{27}$ molecules s^{-1}. From a second analysis of the same SO_2^+ density profile by Crary and Bagenal (2000) using a simpler monoenergetic velocity of 2.48 km s^{-1} for the source of SO_2 at Io's exobase, a similar SO_2 escape rate of a $1\text{-}3.5 \times 10^{27}$ molecules s^{-1} was suggested. If the SO_2 exobase source rate is indeed this large and if the exothermic products are not very energetic so as not to dilute their

local circumplanetary density contributions, then SO_2 may possibly provide an additional significant contribution to the Iogenic plasma source in the Outer Region. Information regarding the electron impact cross-sections and their exothermic energy distributions for the products in the molecular dissociation of SO_2 (and SO) is needed to address this question.

5. SUMMARY

The instantaneous pickup ion rates for the Iogenic plasma source created O and S in the Outer Region through electron impact and charge exchange processes in the plasma torus have been calculated in three dimensions on a circumplanetary scale for one location of Io in System III longitude and local time. The pickup ion rates for O and S are presented in two-dimensional distributions by integrating the three-dimensional rates along the magnetic field line. Similar two-dimensional distributions for a number of volumetric quantities determined from these pickup ion rates are presented for the net-mass and total mass loading rates, the mass per unit magnetic flux rate, the pickup conductivity, the radial pickup current, and the net-energy loading rate for the plasma torus. All of the two-distributional distributions are highly peaked at Io's location and hence highly asymmetric about Jupiter. The physical origin and the amount of asymmetry for the volumetric quantities are discussed. The spatially integrated rates for the net-mass and total mass loading rates are 154 kg s^{-1} and 277 kg s^{-1}, respectively, with 71% of the rate confined to a very large peak located within ±20° longitude of Io's orbital location. The spatially integrated rate for the mass per unit magnetic flux is 1.1 x 10^8 kg s^{-1} T^{-1}. Maximum values for the pickup conductivity and the radial pickup current at Io's location are 2.5 x 10^{-3} mho and 4 x 10^4 amps. The spatially integrated net-energy loading rate is 1.03 x 10^{12} watts and is dominated by the contributions from the peak centered on Io.

The space-time variability of the Iogenic plasma source is discussed and is shown to depend upon the complete time history of the neutral clouds from which they are created. The Iogenic plasma source calculated here for the Outer Region is compared to various estimates for the Iogenic plasma source created in the combined Inner and Outer Regions, and the mass source rate for the Inner Region (~300-700 kg s^{-1}) is estimated to be ~1 to 2.5 times larger than that calculated for the Outer Region (277 kg s^{-1}). Other possible sources of pickup ions for the Outer

Region are also discussed. The Inner Region is therefore expected to be the dominant contributor of ions to the formation of the plasma torus ribbon, the maximum density peak in the radial structure of the plasma torus, and a comparable if not larger contributor to the energy budget of the plasma torus compared to the Outer Region. Future improvements in calculating the Iogenic plasma source include the addition of near-Io plasma effects in the satellite flank and plasma wake and the more complete specification of source rates for neutrals at Io's exobase.

Acknowledgments. The research was sponsored by the National Aeronautical and Space Administration through the Magnetospheric Physics Program under contract NASW-97032 to AER.

REFERENCES

Bagenal, F. (1997) The ionization source near Io from Galileo wake data, *Geophys. Res. Letts. 24*, 2111-2114.

Brown, R.A. (1981) The Jupiter Hot Plasma Torus: Observed Electron Temperature and Energy Flow, *Ap. J. 244*, 1072-1080.

Combi, M.R., K. Kabin, T.I. Gombosi, and D.L. DeZeeuw (1998) Io's plasma environment during the Galileo flyby: Global three-dimensional MHD modeling with adaptive mesh refinement, *J. Geophys. Res. 103*, 9071-9081.

Crary, F.J. and F. Bagenal, Ion Cyclotron Waves, Pickup Ions, and Io's Neutrals (2000) *J. Geophys Res. 105*, 25,379-25,389.

Delamere, P.A., W.H. Smyth and M.L. Marconi (2001) Transport Studies of the Radial and Longitudinal Structure in the Plasma Torus, paper presented at the meeting Jupiter: Planet, satellites and Magnetosphere, Boulder Colorado, June 25-30, 2001.

Frank, L.A., W.R. Paterson, K.L. Ackerson, V.M. Vasyliunas, F.V. Coroniti, and J.S. Bolton (1996) Plasma Observations at Io with the Galileo Spacecraft, *Science 274*, 394-395.

Goertz, C.K. (1980) Io's Interaction with the Plasma Torus, *J. Geophys. Res. 85*, 2949-2956.

Gurnett, D.A., W.S. Kurth, A. Roux, S.J. Bolton, and C.K. Kennel (1996) Galileo Plasma Wave Observations in the Io Plasma Torus and Near Io, *Science 274*, 391-392.

Hill T. W. and D.H. Pontius (1998) Plasma Injection near Io, *J. Geophys. Res. 103*, 19,879-19,885.

Huddleston, D.E., R.J. Strangeway, J. Warnecke, C.T. Russell, and M.G. Kivelson (1997) Ion Cyclotron Waves in the Io Torus during the Galileo Encounter: Warm Plasma Dispersion Analysis, *Geophys. Res. Letts. 24*, 2143-2146.

Kabin,. M.R. Combi, T.I. Gombosi, D.L. DeZeeuw, K.C. Hansen, and K.G. Powell (2001) Io's Magnetospheric interaction: an MHD model with day-night asymmetry, *Planet. Space Sci. 49*, 337-344.

Kivelson, M.G., K.K. Khurana, R.J. Walker, J. Warnecke, C.T. Russell, J.A. Linker, D.J. Southwood, and C. Polanskey (1996) Io's Interaction with the Plasma Torus: Galileo Magnetometer Report, *Science 274*, 396-398.

Linker, J.A., K.K. Khurana, M.G, Kivelson, and R.J. Walker (1998) MHD Simulations of Io's Interaction with the Plasma Torus, *J. Geophys. Res. 103*, 19,867-19877.

Linker, J.A., R. Lionello, M.G. Kivelson, and R.J. Walker (2001) Io's Magnetic and Plasma Environment, paper presented at the meeting Jupiter: Planet, satellites and Magnetosphere, Boulder Colorado, June 25-30, 2001.

Marconi, M.L.and W.H. Smyth (1996) Io Plasma Torus: Nature of the Iogenic Plasma Source, *BAAS 28*, 1154-1155.

McGrath, M.A. and R.E. Johnson (1989) Charge exchange cross sections for the Io plasma torus, *J. Geophys. Res. 94*, 2677-2683.

Morgan, J.S. (1985a) Temporal and Spatial Variations in the Io Torus, *Icarus 62*, 389-414.

Morgan, J.S. (1985b) Models of the Io Torus, *Icarus 63*, 243-265.

Oliversen, R.J., F. Scherb, W.H. Smyth, M.E. Freed, R. C. Woodard, M.L. Marconi, K.D. Retherford, O.L. Lupie, and J.P. Morgenthaler (2001) Sunlit Io Atmospheric [O I] 6300 Å Emission and the Plasma Torus, *J. Geophys. Res.*, in press.

Pilcher, C.B., Smyth, W.H., Combi, M.R., and Fertel, J.H. (1984) Io's Sodium Directional Features: Evidence for a Magnetospheric-Wind-Driven Gas Escape Mechanism, *Ap. J. 287*, 427-444.

Pontius, D.H., R.A. Wolf, T.W. Hill, R.W. Spiro, Y.S. Yang, and W.H. Smyth (1998) Velocity Shear Impoundment of the Io Plasma Torus, *J. Geophys. Res. 103*, 19,935-19,946.

Saur, J., F.M. Neubauer, D.F. Strobel and M.E. Summers (1999) Three-Dimensional Plasma Simulations of Io's Interaction with the Io Plasma Torus: Asymmetric Plasma Flow, *J. Geophys. Res. 104*, 25,105-25,126.

Scherb, F. and W.H. Smyth (1993) Variability of [O I] 6300-Å Emission Near Io, *J. Geophys. Res. 98*, 18729-18736.

Smyth, W. H. (1979) Io's Sodium Cloud: Explanation of the East-West Asymmetries. *Ap. J. 234*, 1148-1153.

Smyth, W. H. (1983) Io's Sodium Cloud: Explanation of the East-West Asymmetries. II. *Ap. J. 264*, 708-725.

Smyth, W.H., Neutral Cloud Distribution in the Jovian System (1992) *Adv. Space Res. 12*, 337-346.

Smyth, W.H. (1998) Energy Escape Rate of Neutrals from Io and the Implications for Local Magnetospheric Interactions, *J. Geophys. Res. 103*, 11941-11950.

Smyth, W.H., and Combi, M.R. (1987) Correlating East-West Asymmetries in the Jovian Magnetosphere and the Io Sodium Cloud, *Geophys. Res. Lett. 14*, 973-976.

Smyth, W.H. and M.R. Combi (1988a) A General Model for Io's Neutral Gas Cloud.I. Mathematical Description, *Ap. J. Supp. 66*, 397-411.

Smyth, W.H. and M.R. Combi (1988b) A General Model for Io's Neutral Gas Cloud.II. Application to the Sodium Cloud, *Ap. J. 328*, 888-918.

Smyth, W.H. and M.R. Combi (1991) The Sodium Zenocorona, *J. Geophys. Res. 96*, 22711-22727.

Smyth, W.H. and M.R. Combi (1997) Io's Sodium Exosphere and Spatially Extended Cloud: A Consistent Flux Speed Distribution, *Icarus 126*, 58-77.

Smyth, W.H. and M.L. Marconi (1998a) An Initial Look at the Iogenic SO_2^+ Source During the Galileo Flyby of Io, *J. Geophys. Res. 103*, 9083-9089.

Smyth, W.H. and M.L. Marconi (1998b) An Explanation for the East-West Asymmetry of the Io Plasma Torus, *J. Geophys. Res. 103*, 9091-9100.

Smyth, W.H. and M.L. Marconi (2000) Io's Oxygen Source: Determination from Ground-based Observations and Implications for the Plasma Torus, *J. Geophys. Res. 105*, 7783-7792.

Smyth, W.H. and M.L. Marconi (2001) Nature of the Iogenic Plasma Source in Jupiter's Magnetosphere II. Near-Io Distribution, paper in preparation.

Smyth, W.H. and M.B. McElroy (1977) The Sodium and Hydrogen Gas Clouds of Io, *Planet. Space Sci. 25*, 415-431.

Smyth, W.H. and M.B. McElroy (1978) Io's Sodium Cloud: Comparison of Model and Two-Dimensional Images, *Ap.J. 226*, 336-346.

Smyth, W.H. and D.E. Shemansky (1983) Escape and Ionization of Atomic Oxygen from Io, *Ap. J. 271*, 865-875.

Smyth, W.H., R.-L. Shia, M.C. Wong, and M.L. Marconi (2001) 2-D Modeling of the Structure, Composition, and Dynamics of Io's Atmosphere, paper presented at the meeting Jupiter: Planet, satellites and Magnetosphere, Boulder Colorado, June 25-30.

Thomas, N. (1996) High Resolution Spectra of Io's Neutral Potassium and Oxygen Clouds, *Astron. Astrophys. 313*, 306-314.

Wong, M.C. and W.H. Smyth (2000) Model Calculations for Io's Atmosphere at Eastern and Western Elongations, *Icarus 146*, 60-74.

Table 1. O and S Loss Processes in the Plasma Torus near Io's Orbit at Western-Elongation

	Relative Rate, %	Lifetime, hours
Atomic Oxygen		
$O + e \rightarrow O^+ + 2e$	21.77	80
$O + O^+ \rightarrow O^+ + O$	67.75	26
$O + O^{++} \rightarrow O^{++} + O$	0.45	3900
$O + O^{++} \rightarrow O^+ + O^+$	0.04	40000
$O + S^+ \rightarrow O^+ + S$	0.09	19000
$O + S^{++} \rightarrow O^+ + S^+$	5.04	350
$O + S^{+++} \rightarrow (O^+)^* + (S^{++})^*$	4.84	360
$O + h\nu \rightarrow O^+ + e$	0.02	38000
Total	100.00	
Atomic Sulfur		
$S + e \rightarrow S^+ + 2e$	60.12	15
$S + S^+ \rightarrow S^+ + S$	19.47	46
$S + S^{++} \rightarrow S^{++} + S$	8.94	100
$S + S^{++} \rightarrow S^+ + S^+$	0.34	2600
$S + S^{+++} \rightarrow S^+ + S^{++}$ $S + S^{+++} \rightarrow S^{++} + S^+$	1.72	520
$S + O^+ \rightarrow S^+(^2P) + O(^3P)$	7.96	110
$S + O^+ \rightarrow S^+(^2D) + O(^1D)$	0.32	2800
$S + O^{++} \rightarrow S^+ + O^+$ $S + O^{++} \rightarrow S^{++} + O^+ + e$	1.01	890
$S + h\nu \rightarrow S^+ + e$	0.12	7520
Total	100.00	

Table 2. Volume Integrated Pickup Ion Rates

Neutral Species	Electron Impact Ionization (10^{27} ions s^{-1})	Charge Exchange (10^{27} ions s^{-1})	Total (10^{27} ions s^{-1})
New Pickup Ion Rates			
O	1.28	3.47	4.75
S	1.75	1.05	2.80
O + S	3.03	4.52	7.55
Net Pickup Ion Rates	3.03	0.82	3.85

Table 3. Net and Total Mass Loading Rates[a]

Magnetospheric Process	Net Mass Loading Rate		Total Mass Loading Rate	
	(kg/s)	(%)[a]	(kg/s)	(%)[a]
Electron Impact Ionization	127	17.3	127	17.3
Charge Exchange	27	3.7	150	20.4
Total:	154	21.0	277	37.7

[a] Based upon the combined O and S exobase upward source rate of 734 kg/s (100%); about 62% of the source rate produces ballistic atom trajectories that are confined to Io's corona.

Table 4. Estimates for the Total Iogenic Plasma Source

Net Mass-Loading		Charge Exchange		Total		
(10^{28} s^{-1})	(kg s^{-1})	(10^{28} s^{-1})	(kg s^{-1})	(10^{28} s^{-1})	(kg s^{-1})	Reference
Neutral Clouds						
0.57	225	1.15	367	1.72	592	Smyth (1992)
	154		510	1.95	664	Smyth and Marconi (2000)
Galileo Flyby						
0.53-1.7	188-600	0	0	0.53-1.7	188-600	Bagenal (1997)
MHD Simulations						
0.8	300 (f)	1.5	540 (f)	2.3	840 (f)	Combi et al. (1998)[a]
1.8	650 (r)	3.2	1150 (r)	5.0	1500 (r)	
0.5	200 (n)	1.5	600 (n)	2.0	800 (n)	Linker et al. (1998)[b]
0.3	120 (m)	0.9	360 (m)	1.2	480 (m)	
1.3	470	1.4	510	2.7	980	Kabin et al. (2001)

[a] The two cases are for fixed (f) and reflective (r) inner boundary conditions about Io.
[b] The two cases are for no (n) intrinsic magnetic field and an assumed (m) intrinsic magnetic field for Io.

Table 5. Spatial Distribution: Total Ion Pickup Loading Rate

	Mass Rate (kg/s)
Iogenic Plasma Source (Outer Region)	
Exobase to the ±20° Base of the Io Peak	197
Remaining 320° of System III Longitude about Jupiter	80
Total Outer Region Source	277
Iogenic Plasma Source (Inner and Outer Regions)	600 –980

FIGURE CAPTIONS

Figure 1. Atomic Oxygen Lifetime in the Plasma Torus at Western Elongation. The electron impact (EI), composite charge exchange (CE), and total (EI + CE) lifetimes, in units of hours, of atomic oxygen are shown in (a), (b), and (c), respectively, in a plasma torus plane located at a local time corresponding to western elongation (dusk ansa) and at a System III longitude of 230°. The radial ($\tilde{L}$) and vertical ($\tilde{z}$) plasmacentric coordinates (Smyth and Combi 1988b) are defined so that the density structure of the plasma are fixed in location and Io moves around the gray oval as a function of System III longitude and at 230° is located at the position of the gray dot.

Figure 2. Atomic Sulfur Lifetime in the Plasma Torus at Western Elongation. Same caption as Fig. Caption 2, except for atomic sulfur.

Figure 3. Incomplete Collisional Cascade Source Velocity Distribution. The source speed distribution (normalized to unit area) adopted for the flux of O and S at Io's exobase is that determined for Io's sodium corona and neutral clouds by Smyth and Combi (1997). The distribution peaks at 0.5 km s^{-1} and has an incomplete collisional cascade tail characterized by the parameter $\alpha = 7/3$ (see text ; also Smyth and Combi 1988b).

Figure 4. Distribution of Atomic Oxygen and Sulfur about Jupiter. For a line of sight perpendicular to Io's orbital plane, the model calculated circumplanetary distribution of the column density (atoms cm^{-2}) is shown for atomic oxygen in (a) and for atomic sulfur in (b). The relative location of Jupiter (half lit disk), Io's orbit (dashed circle), and Io (filled circle, on dashed circle) at western elongation are indicated. Io and the corotational plasma torus both move in the counter clockwise direction with the plasma torus overtaking Io with a relative period of ~13 hrs. The unmarked inner contour is 1.5×10^{12} atoms cm^{-2} in (a) and 2.5×10^{11} atoms cm^{-2} in (b). In (c), column density profiles are shown along the horizontal dashed line in (a) and (b).

Figure 5. Pickup Ion Rates for Atomic Oxygen and Sulfur. The model calculated circumplanetary distribution of the pickup ion rate (ions cm^{-2} s^{-1}) integrated along the magnetic field is shown for electron impact ionization (EI), charge exchange and (CE), respectively, in (a), and (b) as created by atomic oxygen in Figure 4a and in (d) and (e) as created by atomic sulfur in Figure 4b. The unmarked inner contour is 5×10^{6} ions cm^{-2} s^{-1} in (a), (b), (d) and (e). In (c), pickup ion rate profiles for EI and CE processes are shown along the horizontal dashed line in (a) and (b), respectively, while in (f), the same profiles are shown along the horizontal dashed line in (d) and (e), respectively.

Figure 6. Net-Mass Loading Rate. The model calculated circumplanetary distribution for the net-mass loading of the plasma torus corresponding to the combined O and S pickup ion rates in Figure 5 is shown in (a) in two dimensions (kg m-2 s-1), having been integrated along the magnetic field, and in (b) in one dimension (kg s-1 per 5°) as a function of System III longitude, having been integrated, in addition, along the radial coordinate. The relative locations of Jupiter

(half lit disk), Io's orbit (dashed circle), and Io (filled circle, on the dashed circle) at western elongation are indicated. The two outer dashed lines in (a), originating from Jupiter, are centered 20° on either side of the dashed line connecting Jupiter and Io. The locations of these same three dashed lines are also shown in (b) by the three vertical dashed lines and mark the boundaries between which 71% of the spatially-integrated net-mass loading rate of 154 kg s^{-1} is contained. In (a), the unmarked inner and outer contours are 3×10^{-15} kg m^{-2} s^{-1} and 2×10^{-18} kg m^{-2} s^{-1}, respectively.

Figure 7. Total-Mass Loading Rate. Same caption as Fig. Caption 6, except calculated for the total (EI and equivalent CE) mass-loading rate, with the following changes. The inner contour in (a) is 8×10^{-15} kg m^{-2} s^{-1}. The ± 20° boundaries contain 71% of the total spatially-integrated mass-loading rate of 277 kg s^{-1}.

Figure 8. Mass per Unit Magnetic Flux Source Rate. The model calculated circumplanetary distribution for the mass per unit magnetic flux source rate (kg m^{-2} s^{-1} T^{-1}) integrated along the magnetic field and corresponding to the combined O and S pickup ion rates in Figure 5 is shown in two dimensions in (a) and in a one-dimensional profile in (b) that is along the horizontal dashed line in (a). The unmarked inner contours near Io in (a) is 3×10^{-9} kg m^{-2} s^{-1} T^{-1}. The total spatially integrated rate is 1.1×10^{8} kg s^{-1} T^{-1}.

Figure 9. Pickup Conductivity. The model calculated circumplanetary distribution for the height-integrated (integrated along the magnetic field) pickup conductivity (mho) for the combined O and S pickup ion rates in Figure 5 is shown in (a) and a one-dimensional profile in along the horizontal dashed line in (a) is shown in (b). The unmarked two inner contours near Io in (a) are 5×10^{-5} mho and 5×10^{-4} mho.

Figure 10. Radial Pickup Current. The model calculated circumplanetary distribution for the radial pickup conductivity (amps) for the combined O and S pickup ion rates in Figure 5 is shown in two dimensions in Jovicentric coordinates in (a) and in a one-dimensional profile in (b) along the horizontal dashed line in (a).

Figure 11. Net-Energy Loading Rate. The model calculated circumplanetary distribution for the net-energy loading rate (watts m^{-2}) is shown in two dimensions in Jovicentric coordinates in (a) and in a one-dimensional profile in (b) along the horizontal dashed line in (a). The unmarked inner contour is 1 x 10^{-4} watts m^{-2}. The spatially integrated net-energy rate is 1.03 x 10^{12} watts.

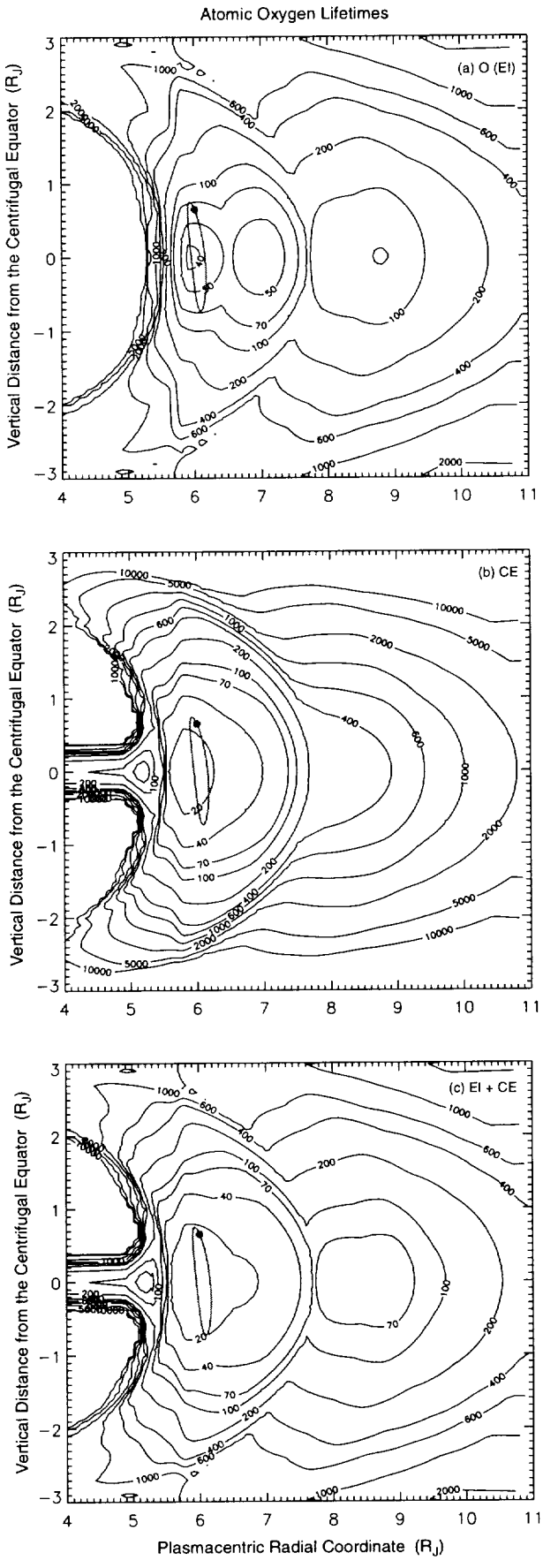
Atomic Oxygen Lifetimes
(a) O (EI)
(b) CE
(c) EI + CE
Vertical Distance from the Centrifugal Equator (R_J)
Plasmacentric Radial Coordinate (R_J)

Figure 1

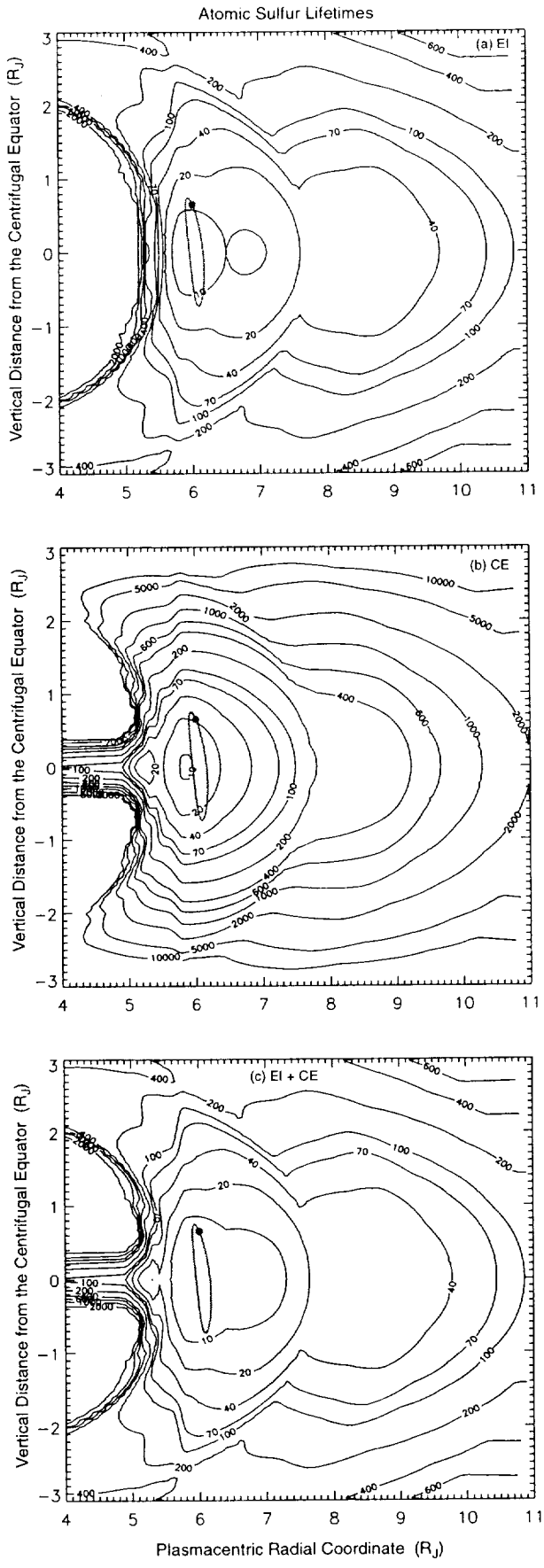
Atomic Sulfur Lifetimes
(a) EI
(b) CE
(c) EI + CE
Vertical Distance from the Centrifugal Equator (R_J)
Plasmacentric Radial Coordinate (R_J)

Figure 2

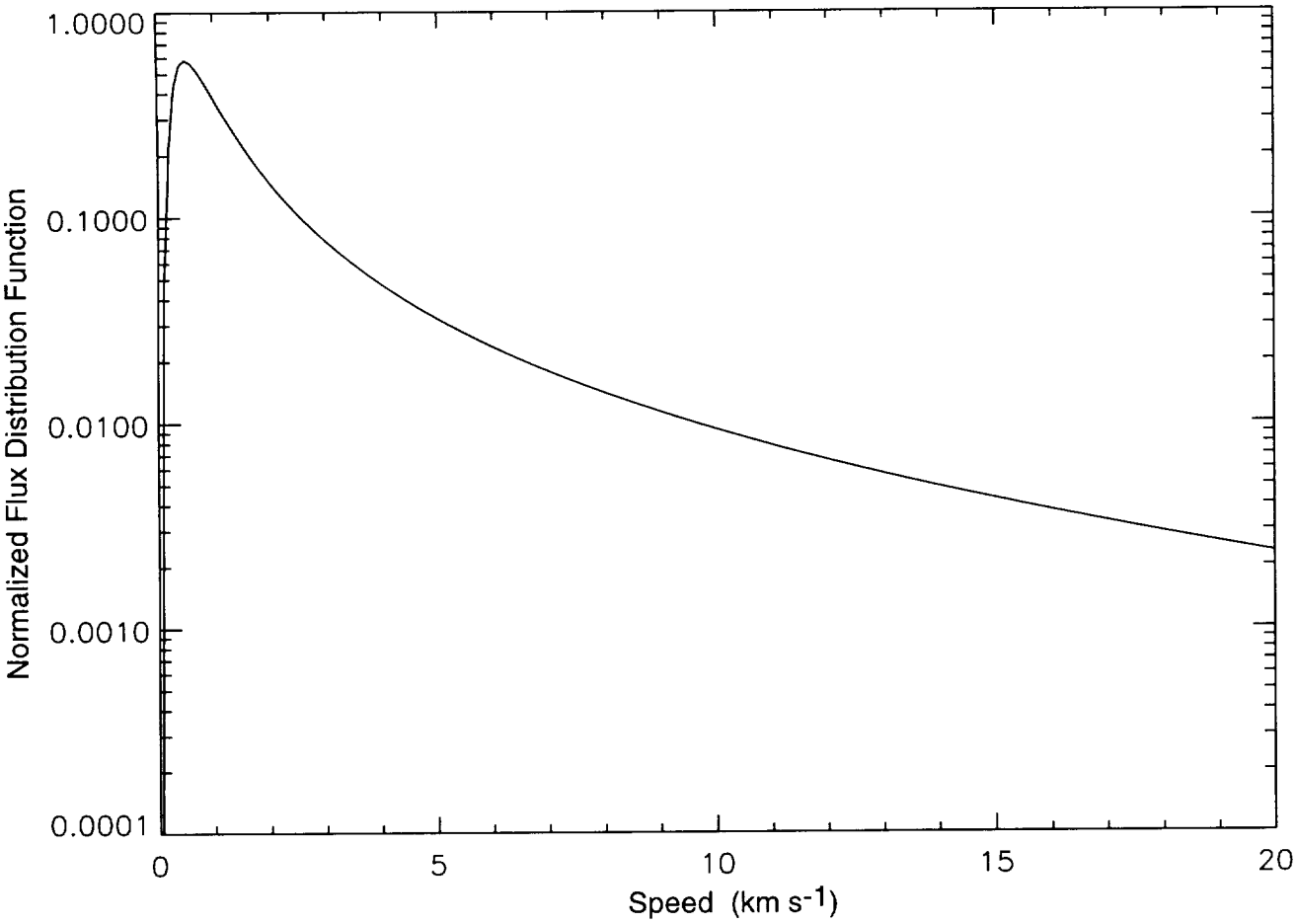
1.0000
0.1000
0.0100
0.0010
0.0001
Normalized Flux Distribution Function
0
5
10
15
20
Speed (km s-1)

Figure 3

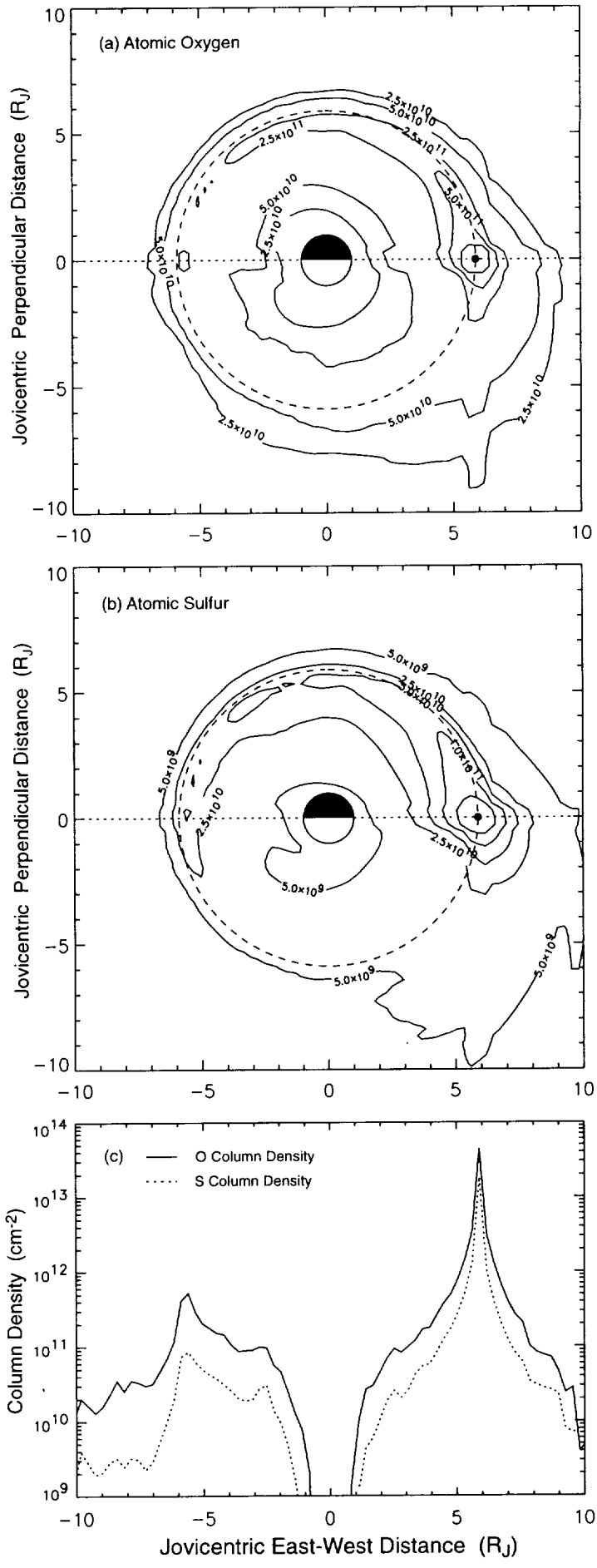
(a) Atomic Oxygen
Jovicentric Perpendicular Distance (R_J)
(b) Atomic Sulfur
Jovicentric Perpendicular Distance (R_J)
(c)
O Column Density
S Column Density
Column Density (cm^{-2})
Jovicentric East-West Distance (R_J)

Figure 4

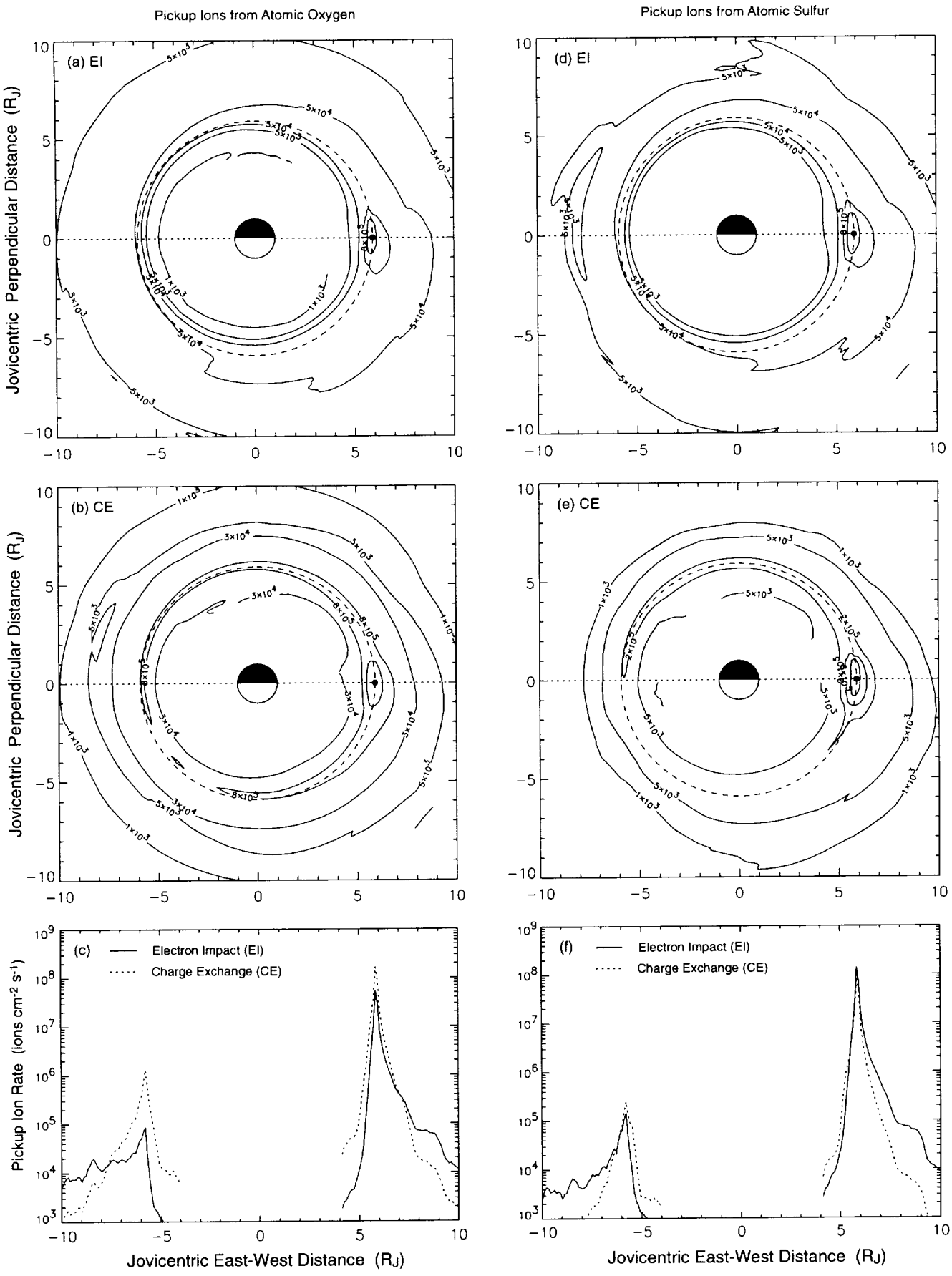
Pickup Ions from Atomic Oxygen
Pickup Ions from Atomic Sulfur
(a) EI
(b) CE
(c)
Electron Impact (EI)
Charge Exchange (CE)
(d) EI
(e) CE
(f)
Electron Impact (EI)
Charge Exchange (CE)
Jovicentric Perpendicular Distance (R_J)
Pickup Ion Rate (ions cm^{-2} s^{-1})
Jovicentric East-West Distance (R_J)

Figure 5

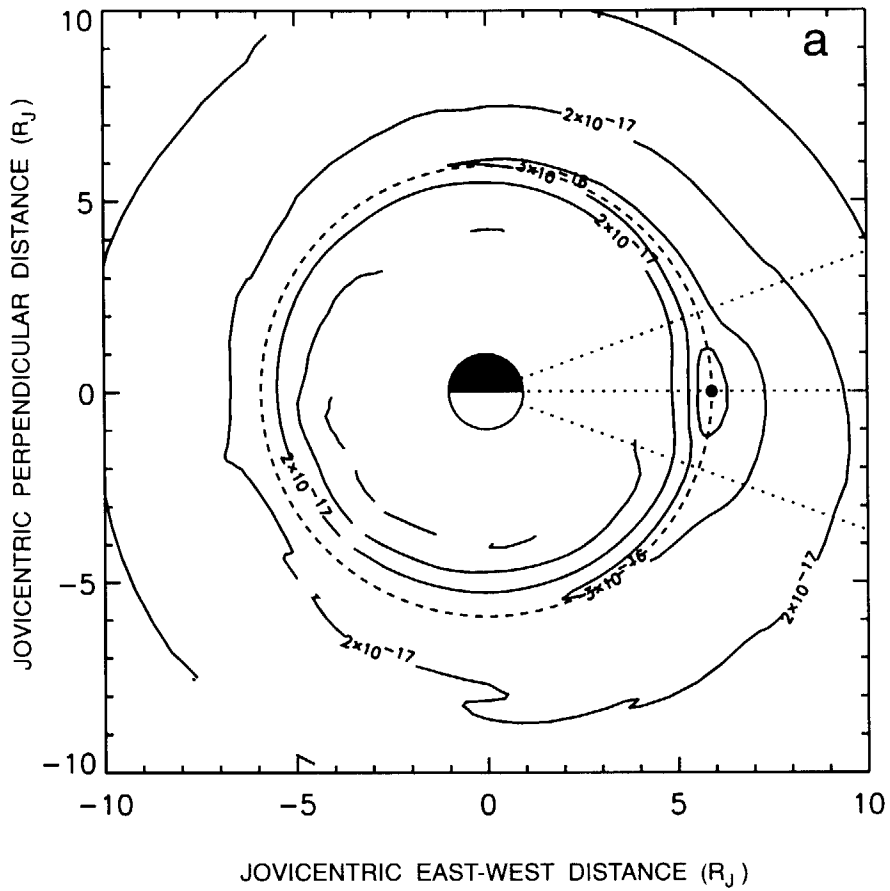
a
JOVICENTRIC PERPENDICULAR DISTANCE (R_J)
JOVICENTRIC EAST-WEST DISTANCE (R_J)
10
5
0
−5
−10
−10
−5
0
5
10
2×10⁻¹⁷
3×10⁻¹⁶
2×10⁻¹⁷
2×10⁻¹⁷
3×10⁻¹⁶
2×10⁻¹⁷
2×10⁻¹⁷

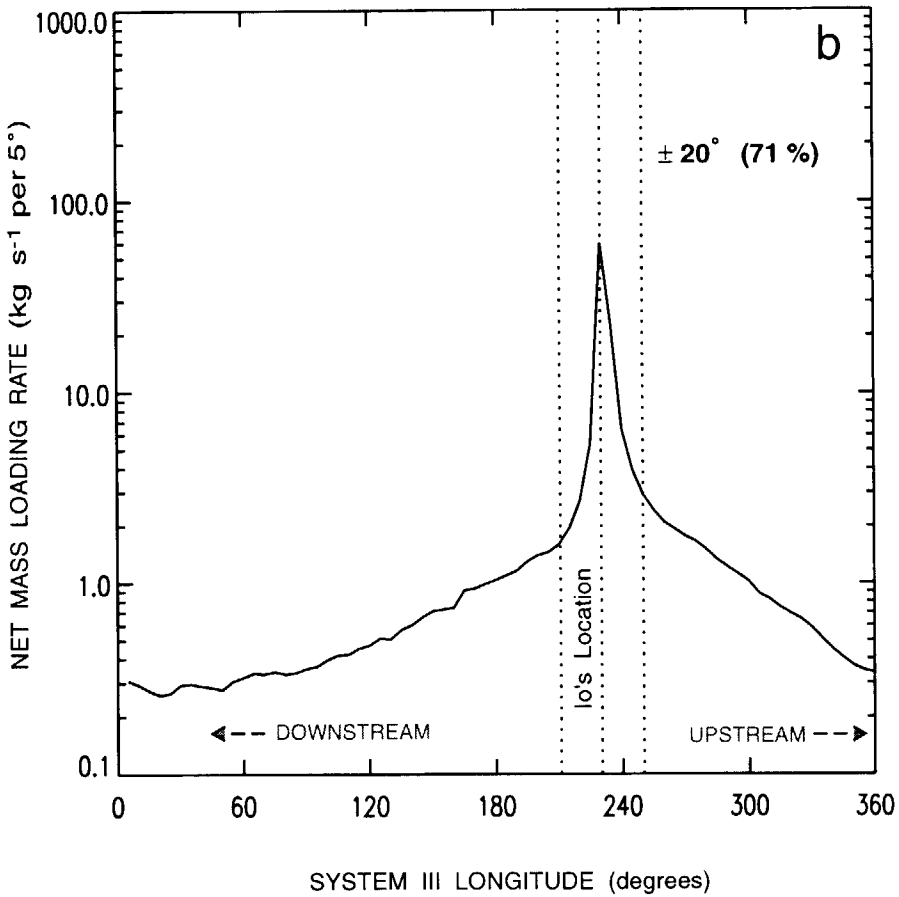
b
NET MASS LOADING RATE (kg s⁻¹ per 5°)
SYSTEM III LONGITUDE (degrees)
1000.0
100.0
10.0
1.0
0.1
0
60
120
180
240
300
360
± 20° (71 %)
Io's Location
DOWNSTREAM
UPSTREAM

Figure 6

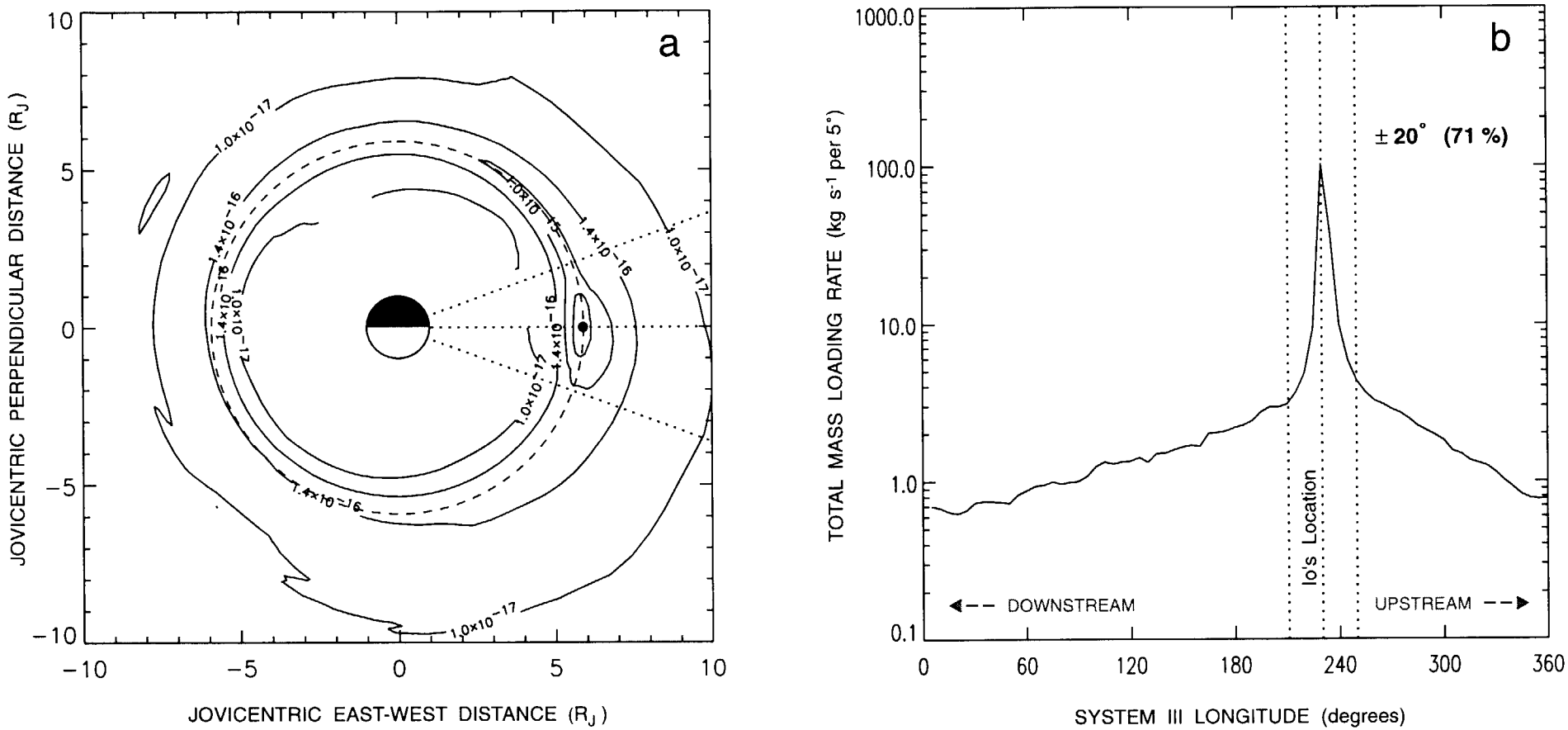
a
b
JOVICENTRIC PERPENDICULAR DISTANCE (R_J)
JOVICENTRIC EAST-WEST DISTANCE (R_J)
TOTAL MASS LOADING RATE (kg s^{-1} per 5°)
SYSTEM III LONGITUDE (degrees)
± 20° (71 %)
Io's Location
DOWNSTREAM
UPSTREAM
1.0×10⁻¹⁷
1.4×10⁻¹⁶
1.0×10⁻¹⁵
1.0×10⁻¹²
10
5
0
−5
−10
1000.0
100.0
10.0
1.0
0.1
0
60
120
180
240
300
360

Figure 7

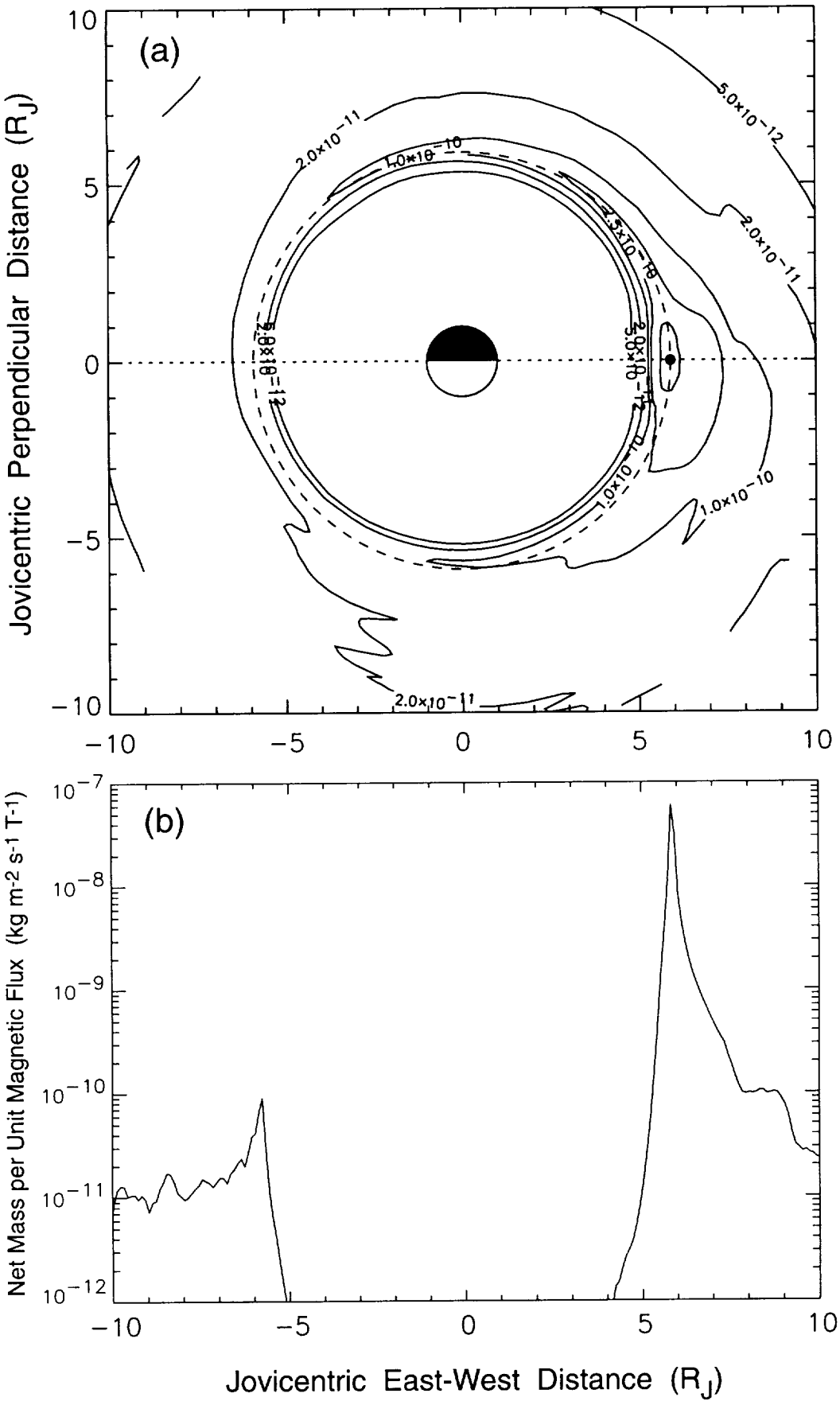
(a)
Jovicentric Perpendicular Distance (R_J)
10
5
0
−5
−10
−10
−5
0
5
10
5.0×10^{-12}
2.0×10^{-11}
1.0×10^{-10}
2.5×10^{-12}
2.0×10^{-11}
5.0×10^{-12}
3.0×10^{-12}
1.0×10^{-10}
1.0×10^{-10}
2.0×10^{-11}
(b)
Net Mass per Unit Magnetic Flux (kg m^{-2} s^{-1} T^{-1})
10^{-7}
10^{-8}
10^{-9}
10^{-10}
10^{-11}
10^{-12}
−10
−5
0
5
10
Jovicentric East-West Distance (R_J)

Figure 8

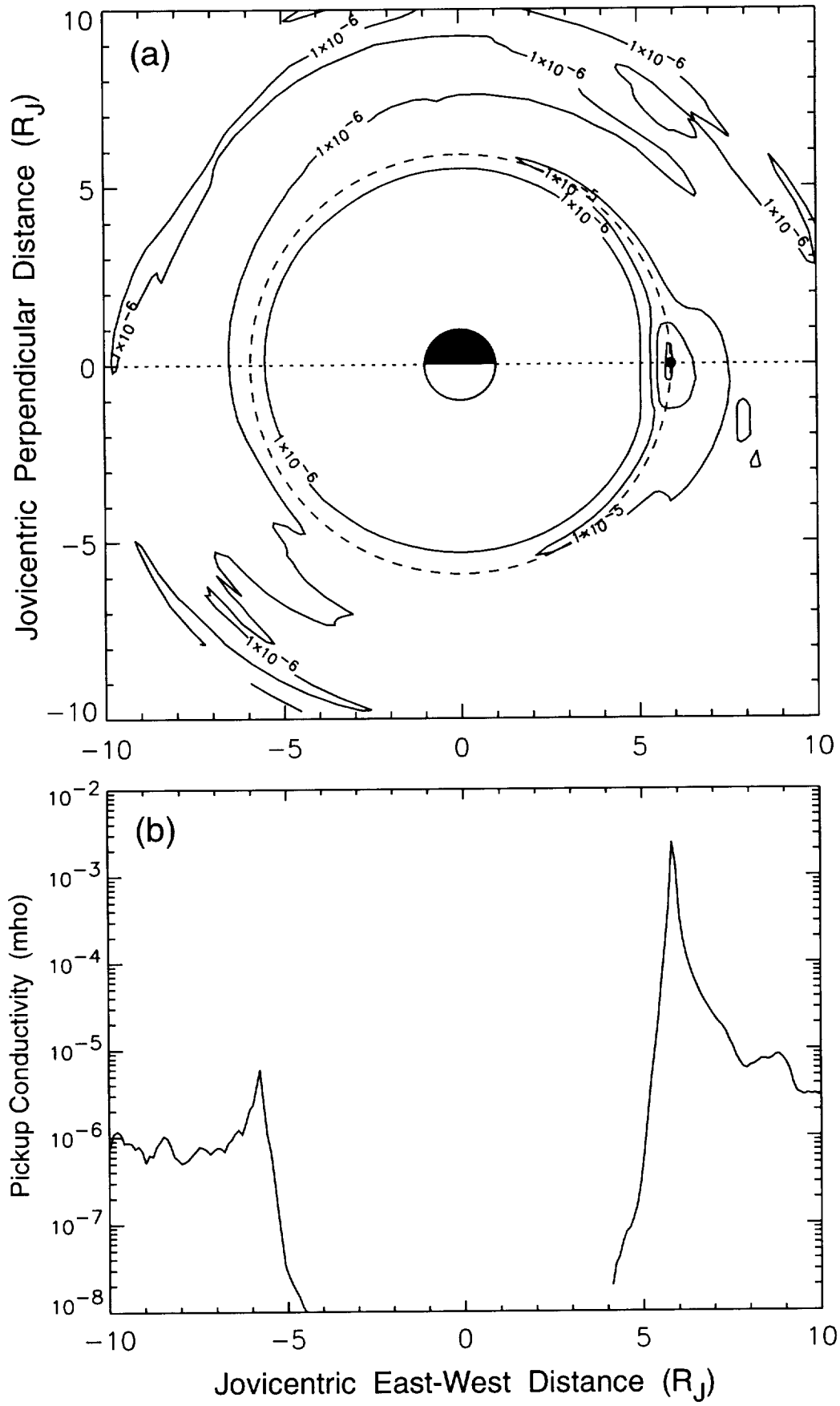
(a)
Jovicentric Perpendicular Distance (R_J)
10
5
0
−5
−10
1×10⁻⁶
1×10⁻⁵
(b)
Pickup Conductivity (mho)
10^{-2}
10^{-3}
10^{-4}
10^{-5}
10^{-6}
10^{-7}
10^{-8}
Jovicentric East-West Distance (R_J)

Figure 9

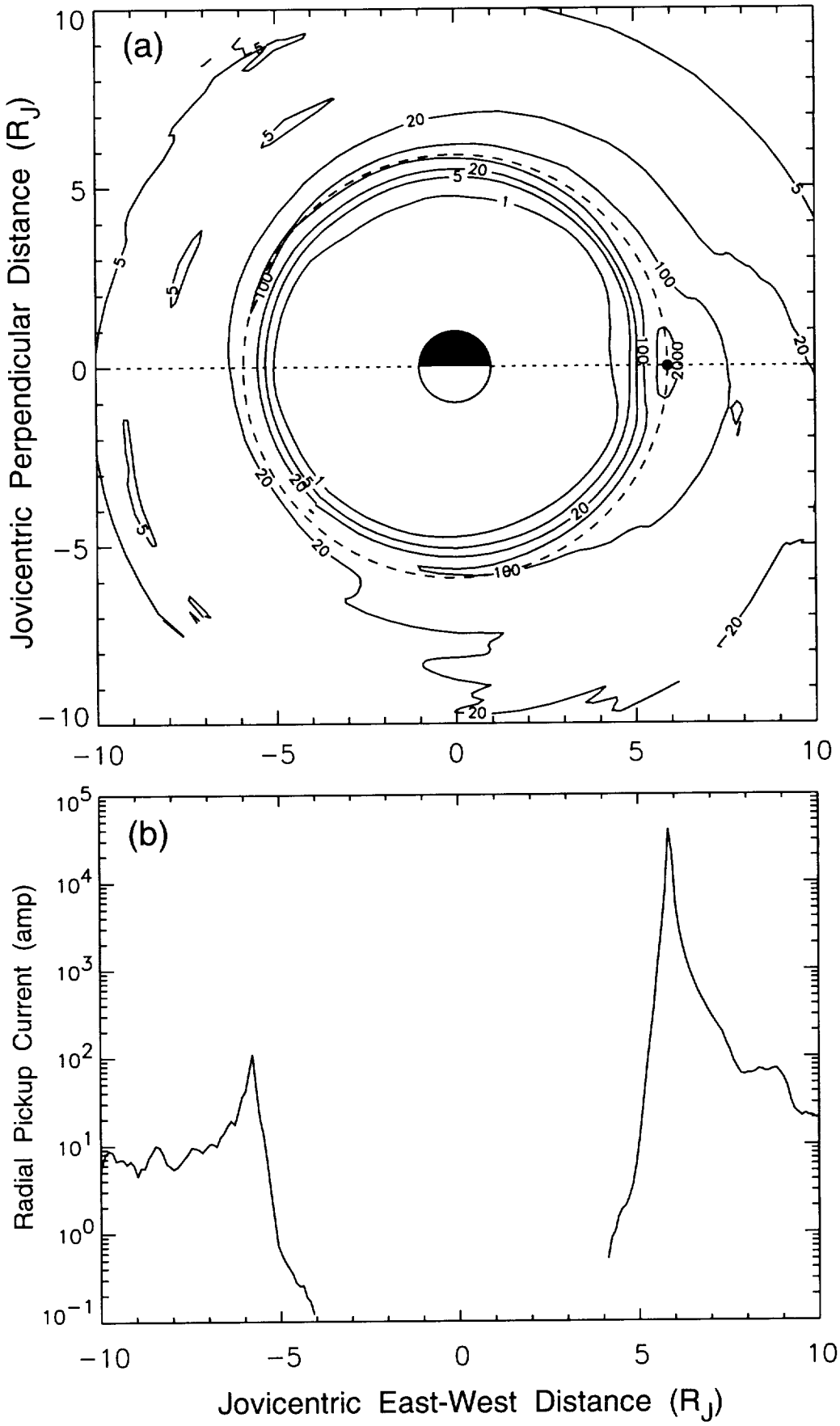
(a)
Jovicentric Perpendicular Distance (R_J)
10
5
0
−5
−10
−10
−5
0
5
10
20
5
1
100
2000
(b)
Radial Pickup Current (amp)
10^5
10^4
10^3
10^2
10^1
10^0
10^{-1}
Jovicentric East-West Distance (R_J)

Figure 10

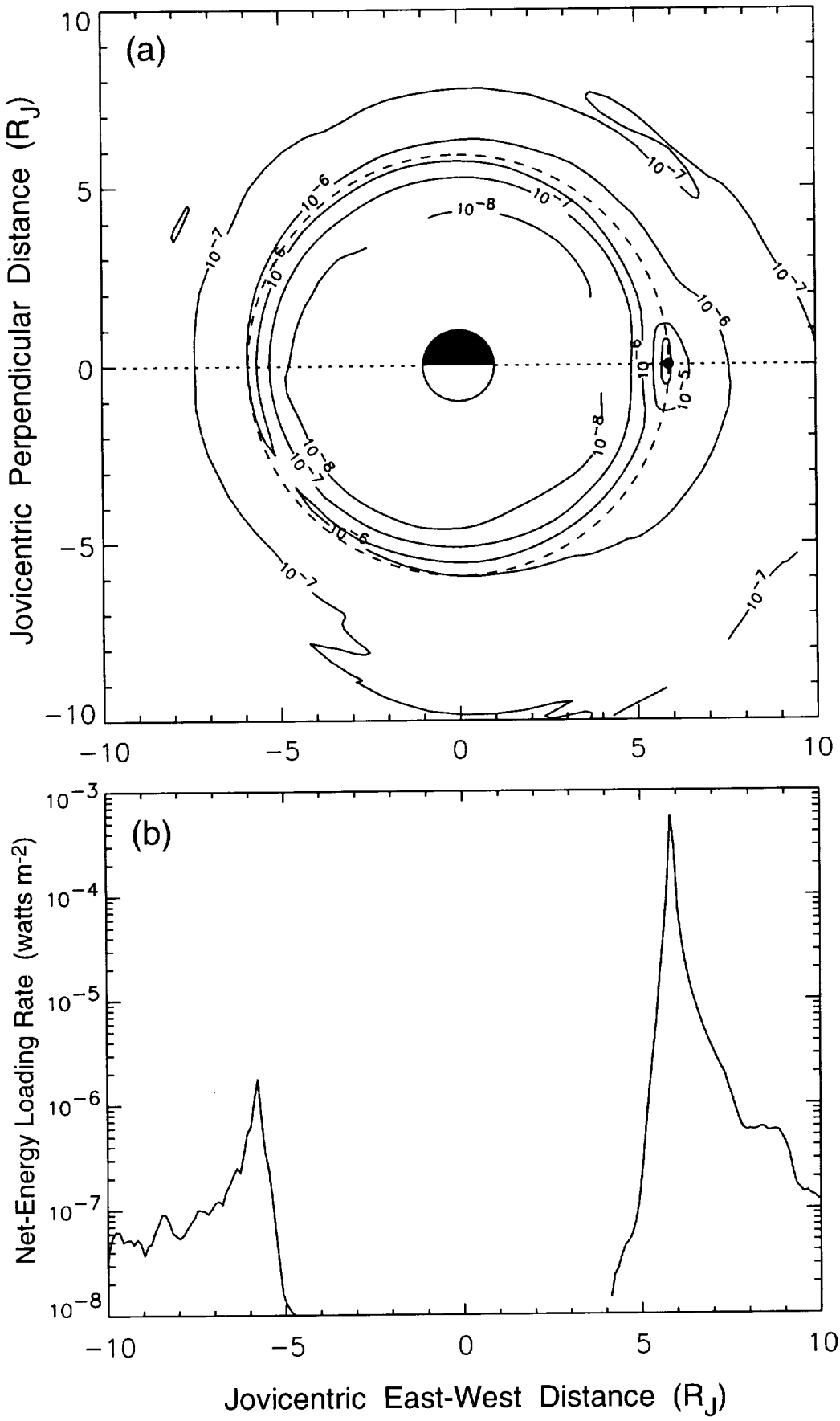
(a)
Jovicentric Perpendicular Distance (R_J)
10
5
0
−5
−10
10^{-5}
10^{-6}
10^{-7}
10^{-8}
(b)
Net-Energy Loading Rate (watts m^{-2})
10^{-3}
10^{-4}
10^{-5}
10^{-6}
10^{-7}
10^{-8}
−10
−5
0
5
10
Jovicentric East-West Distance (R_J)

Figure 11

REPORT DOCUMENTATION PAGE

Form Approved
OMB No. 0704-0188

1. AGENCY USE ONLY *(Leave blank)*	2. REPORT DATE	3. REPORT TYPE AND DATES COVERED
	October 8, 2001	Final Report, Sept. 25, 1997 to Sept. 24, 2001

4. TITLE AND SUBTITLE
Iogenic Plasma and its Rotation-Driven Transport in Jupiter's Magnetosphere

5. FUNDING NUMBERS
NASW-97023

6. AUTHORS
William H. Smyth

7. PERFORMING ORGANIZATION NAME(S) AND ADDRESS(ES)
Atmospheric and Environmental Research, Inc.
131 Hartwell Avenue
Lexington, MA 02421-3126

8. PERFORMING ORGANIZATION REPORT NUMBER
P-735

9. SPONSORING/MONITORING AGENCY NAME(S) AND ADDRESS(ES)
NASA Headquarters
Headquarters Contract Division
Washington, DC 20546

10. SPONSORING/MONITORING AGENCY REPORT NUMBER

11. SUPPLEMENTARY NOTES

12a. DISTRIBUTION/AVAILABILITY STATEMENT

12b. DISTRIBUTION CODE

13. ABSTRACT *(Maximum 200 words)*

Model calculations are reported for the Iogenic plasma source created by atomic oxygen and sulfur above Io's exobase in the corona and extended clouds (Outer Region). On a circumplanetary scale, two-dimensional distributions produced by integrating the proper three dimensional rate information for electron impact and charge exchange processes along the magnetic field lines are presented for the pickup ion rates, the net-mass and total-mass loading rates, the mass per unit magnetic flux rate, the pickup conductivity, the radial pickup current, and the net-energy loading rate for the plasma torus. All of the two-dimensional distributions are highly peaked at Io's location and hence highly asymmetric about Jupiter. The Iogenic plasma source is also calculated on a much smaller near-Io scale to investigate the structure of the highly peak rates centered about Io's instantaneous location. The Iogenic plasma source for the Inner Region (pickup rates produced below Io's exobase) is, however, expected to be the dominant source near Io for the formation of the plasma torus ribbon and to be a comparable source, if not a larger contributor, to the energy budget of the plasma torus, so as to provide the necessary power to sustain the plasma torus radiative loss rate.

14. SUBJECT TERMS
Earth rotation, atmospheric angular momentum

15. NUMBER OF PAGES
66

16. PRICE CODE

17. SECURITY CLASSIFICATION OF REPORT	18. SECURITY CLASSIFICATION OF THIS PAGE	19. SECURITY CLASSIFICATION OF ABSTRACT	20. LIMITATION OF ABSTRACT
Unclassified	Unclassified	Unclassified	